

NASA TECHNICAL NOTE



NASA TN D-4737

0.1

NASA TN D-4737

LOAN COPY: RETURN TO
AFWL (WLIL-2)
KIRTLAND AFB, NM

0131274



TECH LIBRARY KAFB, NM

SINGLE-THERMOCOUPLE METHOD FOR DETERMINING HEAT FLUX TO A THERMALLY THICK WALL

by Floyd G. Howard
Langley Research Center
Langley Station, Hampton, Va.



SINGLE-THERMOCOUPLE METHOD FOR DETERMINING
HEAT FLUX TO A THERMALLY THICK WALL

By Floyd G. Howard

Langley Research Center
Langley Station, Hampton, Va.

NATIONAL AERONAUTICS AND SPACE ADMINISTRATION

For sale by the Clearinghouse for Federal Scientific and Technical Information
Springfield, Virginia 22151 - CFSTI price \$3.00

SINGLE-THERMOCOUPLE METHOD FOR DETERMINING HEAT FLUX TO A THERMALLY THICK WALL

By Floyd G. Howard
Langley Research Center

SUMMARY

A method that accounts for variable thermal properties has been developed for determining heat flux from a single temperature-time history within a thermally thick wall. The accuracy depends on the thermal depth of the measurement point, and ranges from good to excellent for a number of practical cases, with best results occurring for temperature measurements nearest the heated surface in conjunction with a small computing interval. The method is believed to be as accurate, if not more so, than other available methods utilizing multiple thermocouples. If measurement is near the heated surface and accurate, the method can detect sudden changes in slope of heat flux such as are experienced when boundary-layer flow becomes transitional or when heating-rate history fluctuates as a result of body motions in flight.

INTRODUCTION

One problem of considerable importance in the field of heat transfer is that of determining, with a reasonably high degree of accuracy, the heat flux to a calorimeter from measured temperatures. This problem is commonly referred to as the inverse problem. When the total (time-integrated) heat load permits the use of a thin-wall calorimeter, the task of determining the heat-flux history is not a very difficult one. However, when test conditions necessitate a thick-wall calorimeter, the task becomes much more complex. In the thick-wall calorimeter, the variations through the wall of the time derivative of the temperature, the temperature itself, and the temperature-dependent properties (namely conductivity and specific heat) are significant and cannot be neglected as in the thin-wall calorimeter.

A number of methods for calculating heating rates from measured temperatures have been developed (see refs. 1 to 12). However, most of these solutions assume constant thermal properties and therefore have inherent inaccuracies in most practical cases, where temperatures vary over a wide range. The method developed in reference 2 for the reduction of Project Fire calorimeter data does account for variable thermal properties; however, it does have some disadvantages, the major one being that it

requires data from several thermocouples in depth. The disadvantage of this method, when a practical number of thermocouples (like four) are used, is that all thermocouples must function properly in order to obtain accurate data.

The realization of the need for an alternate method that could render valid data analysis if temperature data were not obtained from all thermocouples prompted an investigation which led to the development of the new method reported herein. This method can determine heat flux from the temperature-time history measured at only one depth. Therefore, data from a greater number of stations can be obtained when the total number of thermocouples is limited. The method accounts for variable thermal properties (as functions of temperature) and can account for the effects of radiation losses or a composite wall. It is believed to be as accurate if not more so than other known methods and can probably be modified to account for a coolant gas being blown through a porous wall.

SYMBOLS

A	area, centimeter ²
\bar{A}	square coefficient matrix
\bar{B}	column vector
c	specific heat of wall material, joules/gram-°K
E_T	temperature error ($T_{com} - T_{input}$), °K
k	thermal conductivity of wall material, watts/centimeter-°K
q	heat flux, watts/centimeter ²
q_E	erroneous heat flux, watts/centimeter ²
R	radius of Fire II forebody calorimeter shield (ref. 3) measured perpendicularly from axis of symmetry, centimeters
s	radial distance measured perpendicularly from axis of symmetry of Fire II reentry vehicle (ref. 3), centimeters
T	temperature, °K

T'	temperature at beginning of computing time interval, $^{\circ}\text{K}$
t	time, seconds
Δt	computing time interval, seconds
X	unknown column vector
ϵ	emissivity
ρ	density of wall material, grams/centimeter ³
σ	degree of data scatter; Stefan-Boltzmann constant, 5.6697×10^{-12} watts/centimeter ² -($^{\circ}\text{K}$) ⁴
τ	depth from heated surface to center of block, centimeters
$\Delta\tau$	block thickness in thermal model, centimeters
τ_t	total wall thickness, centimeters

Subscripts:

1,2,3,4	thermocouple (TC) number; time-interval number; block number
com	computed on basis of assumed q
input	input or desired
m	mean value

PROCEDURE AND MECHANICS OF NEW METHOD

Solution for the heat flux is found by using a direct thick-wall heating computer program which computes temperatures for a given heating-rate history (see appendix). The wall thickness is assumed to be divided into a number of blocks, and a finite-difference computational technique is used to compute the temperature of each block. A modification to this program provides for iteration on an assumed heating rate during a short computing time interval to find the value required to produce a known temperature

rise at a particular depth. The iteration is very rapid since the computed temperature error (i.e., the difference between the computed temperature rise based on the assumed heat flux and the desired temperature rise) will vary linearly with the magnitude of the assumed heat flux. Therefore, a linear interpolation or extrapolation of two assumed values of heat input and their associated temperature errors provides the required value of heat input for temperature error of zero, as illustrated in detail in figure 1.

The solid line in the plot of temperature as a function of time (fig. 1(a)) represents a known temperature-time history at some known depth in the wall (τ). First, an assumed heat flux (indicated by the circle marked 1 in fig. 1(b)) is used to compute the temperature rise over the time interval. This temperature rise (indicated by the circle marked 1 in fig. 1(a)) is in error E_T at the end of the time interval. This temperature error as a function of the assumed heat flux is indicated by the circle marked 1 in figure 1(c). The procedure is repeated with a second assumed value of heat flux (indicated by the square marked 2 in fig. 1(b)) to provide a second temperature error as a function of heat flux. This second temperature error is indicated by the square marked 2 in figure 1(c). If thermal properties are held constant for the small computing time interval (Δt) as is done in the finite-difference heating program, the heat flux varies linearly with the temperature error at any depth in the wall. Therefore, two assumed values of heat flux and their associated temperature errors can provide a third and correct value of q at $E_T = 0$ by linear interpolation or extrapolation. In order to provide the correct temperature for each block in the wall, the computations of temperature rise are repeated with this correct heat flux used. The correct temperature is then used to start the computations for the next time interval. This procedure is repeated in order to obtain a solution for q for each time interval. In the example shown in figure 1, the solutions determined from the heat-flux assumptions 1 and 2, 4 and 5, and 7 and 8 are indicated by the solid triangles marked 3, 6, and 9, respectively, in figures 1(b) and 1(c). Since the heating rates are held constant over the computing time interval in the finite-difference computations in the thick-wall program, the solution obtained is a step-changing function as indicated by the heavy, solid horizontal lines in figure 1(b). In order to obtain a smoothly changing value of heat rate (q), the solution for each time interval should be considered to occur as an instantaneous value at the center of the interval, as indicated by the line faired through the solid triangles in figure 1(b). With the exception of the first time interval, the first assumed value of q is always taken to be a 25-percent increase over the correct value determined for the previous time interval (the user must provide the first assumption for the very first interval in order to start the computations). The second value of q is always a 25-percent increase over the first assumption. This increase of 25 percent, however, is arbitrary. Changing this arbitrary increase to 5 percent was investigated and found to have no effect.

The basic inputs required for the single-thermocouple inverse program, in addition to those required for the direct thick-wall heating program (initial temperature gradient through the wall, material properties, dimensions, etc.), are the measured temperature-time history, the depth of the measurement (identified by the number of the block that has the proper depth in the thermal model), and the initial assumed heat flux for the first computing interval. The outputs are the computed heat-flux history and the temperature history for each block.

If the thick wall of a flight vehicle is subjected to heating before the start of computations, the initial temperature gradient through the wall will not be defined by only one thermocouple in depth. If it is desirable to start the inverse computations at some time when $\frac{dT}{dt} \neq 0$ (and therefore $\frac{dT}{d\tau} \neq 0$), a temperature gradient through the wall can be assumed. The effects of an erroneous but reasonable initial temperature gradient will diminish very quickly.

All the computations shown in the present report were obtained by the technique described in this section. However, based on the findings in this report, a more recent program that solves directly for the heat flux without an iteration has been written. The reason q can be solved for directly is explained briefly in the appendix. This factor, however, is important only in regard to machine time and has no significant bearing on the accuracy of the computations.

ANALYSIS AND RESULTS

Analytical Investigation

The validity and accuracy of the single-thermocouple inverse method were analytically investigated by comparing results from the method with known heat inputs. This investigation was conducted by computing the temperatures through a 1.524-cm-thick beryllium wall, divided into 30 blocks to provide an accurate thermal model. The thermal properties used for beryllium are shown in figure 2. Figure 3 shows the geometrical details of the 1.524-cm-thick thermal model, namely the thickness of each block and the depth of the block center or node from the heated surface. Thinner blocks are used near the heated surface because of the large temperature gradients which exist in this region at high heating values. In order to obtain the temperature close to the back surface, thin blocks were used in this region also. With an assumed heat-flux history as input, the basic direct thick-wall heating computer program provided a temperature history for each block. Then it was assumed that a temperature-history measurement was made at only one depth in the wall. This temperature history and the depth at which it occurred, specified by block number, were used as inputs to the single-thermocouple inverse program. The heat flux computed by the inverse method was compared with the input heat

flux. This comparison was made for three different types of heat-flux histories – namely, a smoothly changing one representative of a reentry flight test at zero angle of attack, a step-input heat-flux history representative of a test in a ground facility, and an oscillating heat-flux history that might result from a flight test with significant body motions.

In order to ascertain that the thermal model used in the analytical investigation was divided into a sufficient number of blocks (30), the effect of the number of blocks on accuracy was investigated.

First, the smoothly changing heat-flux history was used in the direct program with an 11-block model, a 30-block model, and a 70-block model. All models were 1.524 cm thick, and the computing time interval was 0.05 second. Temperature-time histories at identical depths were compared and found to be in very close agreement. For example, at 13 seconds the temperature at the 0.254-cm depth was 1424.77° K for the 11-block model and 1420.67° K for the 30-block model after a rise of over 1080° K. Because of the long computer time required for the 70-block model, the run for that model was terminated at 4.4 seconds. The temperature at the 0.254-cm depth was 387.34° K, 387.46° K, and 387.56° K for the 70-, 30-, and 11-block models, respectively, after a rise of over 53° K.

Next, in order to be sure that a 30-block model was also sufficient for the single-thermocouple inverse solution, the temperature-time history at the 0.254-cm depth was used in inverse solutions for the 11-block thermal model and then for the 30-block model. The computed heat-flux histories obtained by using the two different thermal models and a computing time interval of 0.1 second in the inverse solution (with the use of the same temperature history) differed by less than 0.3 percent. It was concluded that the 30-block model gave sufficiently fine thermal detail and that any increase in the number of blocks would have insignificant effect on the results.

The first of the three different heat-flux histories used in the investigation is shown in figure 4. This history represents the heating on a reentry-flight-test vehicle with zero trim and no oscillatory angle of attack. The time at which boundary-layer transition was assumed to begin is noted. The temperatures at four depths that result from this heating are also shown in the figure.

It should be noted that in figure 5, which shows solutions by the single-thermocouple inverse method, beryllium would start to melt at the surface at approximately 11.8 seconds for the heat flux shown. However, in order to analyze the method during and after the time of maximum heat flux, a hypothetical case has been assumed in which melting has been disregarded and thermal properties above melting temperature have been held constant (held at melting-temperature values).

Figure 5(a) shows the effect of computing interval (0.1, 0.2, 0.25, and 0.5 second) at a measurement depth τ of 0.0254 cm. The agreement between the computations and the exact input becomes better as the computing interval is decreased from the largest interval to the smallest interval. Figure 5(b) shows the effect of computing interval (0.2 and 0.5 second) at a measurement depth τ of 0.2540 cm. At this deeper location, computations by use of the 0.2-second interval show a tendency to oscillate during increasing heat flux. The oscillations become more noticeable after maximum heating. Although they are not shown in figure 5(b), computations for a computing interval of 0.1 second at $\tau = 0.2540$ cm were made and found to oscillate a little more than those for a computing interval of 0.2 second, whereas computations for the 0.5-second interval show no indication of oscillation and are in good agreement with the exact input. In the finite-difference computer program the thermal properties (which actually vary instantaneously with temperature) are held constant over the computing interval at their values corresponding to temperature at the beginning of the interval (T'). This practice obviously is a source of error (which is small for examples shown). Therefore when temperature (and thus thermal properties) are changing rapidly, it is apparent that the accuracy will improve with the use of small computing intervals. However, for the finite-difference computing technique, oscillations in the computed heat flux result if the computing interval is too small for a particular thermal depth (dependent on measurement depth and thermal properties).

The frequency at which the temperatures are provided also has influence on the magnitude and pattern of the oscillations because constant slope $\left(\frac{dT}{dt}\right)$ is assumed between the provided points. Figure 6 shows how the computing interval and the frequency at which temperature is provided affect the oscillation of computations for a depth τ of 0.6096 cm (40-percent depth) in a 1.524-cm-thick wall. Computations based on temperatures provided every 0.4 second are shown by the circles for computing intervals of 0.1, 0.2, and 0.4 second in figures 6(a), 6(b), and 6(c), respectively. Oscillations occur for both the 0.1- and 0.2-second computing intervals and tend to diverge at maximum heating. No significant oscillations occur for the 0.4-second computing interval (which corresponds to the frequency at which temperatures were provided). However, some disagreement (5-percent maximum difference between the computed values and the exact input) is noticeable. (It should be noted that the heat-flux scale starts at 500 watts/cm².) Results of computations with temperature inputs at 0.1- and 0.2-second intervals, corresponding to the computing intervals, are shown by the square symbols in figures 6(a) and 6(b). The oscillations are reduced significantly for the computing interval of 0.1 second and are essentially eliminated up to time of maximum heat flux for the computing interval of 0.2 second. Apparently, oscillations in solutions for q are sensitive to the magnitude of the steps of $\frac{dT}{dt}$ at the times of temperature inputs (particularly for measurements

at large depths) and therefore can be minimized by providing temperature inputs for every computing interval.

It should be realized that an oscillating heat flux to the surface may not cause oscillations in the temperature history at a depth in the wall (not at the heated surface). Therefore, it is believed that an absolute unique solution cannot be obtained without surface temperature, since an oscillating heat flux or a smoothly changing one may produce the same temperature-time history at a measurement depth not at the heated surface. Only at the heated surface, where the response time is zero, does a temperature history dictate one and only one heat-flux history, and many solutions which oscillate about some mean solution may exist for measurements at locations other than the heated surface. The oscillations tend to diminish or become less pronounced as the thermal depth becomes less. Therefore from this point of view, the most desirable thermocouple location is as near the heated surface as possible. Presently no suitable governing criteria have been established to determine the smallest computing time interval that can be used for a given thermal depth without causing oscillations in the solution. It may be noted that the lack of an absolute unique solution without surface measurement is not peculiar to the single-thermocouple inverse method.

Shown in figure 7 are solutions for a constant or step-input heat flux of 600 watts/cm². A constant heat flux is characteristic of a ground facility. The initial assumed heat flux for the first computing interval was 200 watts/cm². Solutions are for computing intervals of 0.2, 0.4, 0.6, and 0.8 second for each of three depths, 0.0254, 0.2540, and 0.5080 cm. The accuracy is good even for a depth of 0.5080 cm except for a transient period, which is less than 0.5 second. For each of the three depths the accuracy is shown to improve as the computing interval is decreased. One reason is that, as previously mentioned, the thermal-property values for each block are based on the temperature of the block at the beginning of the computing interval and are held constant over the interval. This procedure introduces a source of error, the magnitude of which depends on how much the block temperatures vary over the interval and how much the properties vary with temperature. It is apparent that this source of error could be diminished by extrapolating the block temperatures with time and basing the properties on the value of temperature at the middle of the computing interval.

Because of body motions, flight vehicles may experience an oscillating heat flux rather than a smoothly changing one. The method was analyzed for such a case and the results are shown in figure 8. The oscillating heat-flux history used as the input was determined as follows: (1) the most severe body motions expected of a planned reentry vehicle were determined by a six-degree-of-freedom program; (2) from the body motions, an angle-of-attack history for a particular body location was determined; and (3) the effect of angle of attack on heating was determined by theoretical computations

and used to modify the zero-angle-of-attack heating (shown in fig. 5) and thus produce the oscillating heat-flux history shown in figure 8. Solutions by the single-thermocouple inverse method shown in figure 8 are for computing intervals of 0.05 and 0.10 second at a measurement depth of 0.0254 cm. At this depth there were noticeable although slight oscillations in the temperature history. At a depth of 0.254 cm the temperature history was even less responsive (as would be expected) to the oscillating heat flux; that is, the temperature histories became smoother as depth was increased. Therefore no attempt was made to reproduce the exact oscillating heat flux from a temperature at this depth. The oscillating temperatures at the 0.0254-cm depth were provided at 0.05-second intervals. The agreement shown in figure 8 by the comparison with the exact input indicates the ability of the method to detect sudden changes in the slope of the heat flux if the measurement is near enough to the heated surface that it will respond to the oscillations in the heat flux. It is very important to note that the temperatures put into the inverse solutions for figures 5 to 8 were precise (except for the linear variation assumed between points) – that is, without scatter or bias. This fact is especially important for the oscillating heat flux (fig. 8), since the temperature history at the 0.0254-cm depth had only slight oscillations. The oscillations were within a total bandwidth of less than 10° K during the period of maximum oscillation. It is believed that with current means of obtaining temperature measurements during flight, the oscillations may be undefinable because of scatter, for a case similar to the one shown. However, it should be understood that the shortcoming would be in defining the correct temperature history and not in the single-thermocouple inverse method.

The results shown in figures 5, 7, and 8 indicate that the accuracy of the method ranges from good to excellent, with best results obtained for temperature measurements nearest the heated surface in conjunction with a small computing interval. Although these results were all obtained for a 1.524-cm-thick beryllium wall, it is believed that the trends would apply to other materials and wall thicknesses. No results that include effects of radiation losses or a composite wall are shown. However, the method can account for these effects.

Comparison With Computation by Other Methods

Comparison with integral method of reference 2. – The rate at which heat is stored in a thick wall is equal to the density of the material (ρ) multiplied by the product of specific heat and change in temperature with respect to time $\left(c \frac{dT}{dt}\right)$ integrated from the heated surface to the back surface (ref. 13). If the density of the wall material is treated as a constant, the one-dimensional heat flux can be expressed as

$$q = \rho \int_0^{\tau_t} \left(c \frac{dT}{dt} \right) d\tau \quad (1)$$

The method developed in reference 2 approximates the exact solution of equation (1) by: (1) determining the value of $c \frac{dT}{dt}$ from measured temperatures at four depths in the wall; (2) fitting an analytical expression through the four values; and (3) integrating analytically under the curve to obtain q . The four values of $c \frac{dT}{dt}$ at a particular time (t) indicated by the circles in figure 9 are determined by fitting an analytical expression $f(t)$ to the measured temperature-time history, differentiating the expression to obtain $\frac{dT}{dt}$, and obtaining c as a function of the temperature. The accuracy in computing the heat flux by this method is dependent upon the accuracy of the analytical curve fit of both temperature as a function of time and $c \frac{dT}{dt}$ as a function of τ . This method of approximation by analytical integration (ref. 2) is hereinafter referred to as the integral method.

The squares in figure 10 represent computations by the integral method for a 1.524-cm-thick beryllium wall (three times the thickness used in refs. 2 and 3) with measurement depths of 0.0254, 0.5080, 1.0160, and 1.5176 cm. At the lower heating rates the computations agree with the exact input very well but at the higher heating rates, difference between the computed value and the exact input becomes noticeable. The measurement locations were spaced approximately evenly through the wall. This evenly spaced arrangement is the same as that in references 2 and 3. Because of the large gradients (variation of T and $c \frac{dT}{dt}$; see fig. 11) near the heated surface, it was believed that with the 1.524-cm-thick wall, better results could be achieved by placing the second and third measurement locations nearer the heated surface. The diamonds in figure 10 represent computations by the integral method for measurement depths of 0.0254, 0.3556, 0.8636, and 1.5176 cm. At the lower heating rates the results are essentially the same as for the evenly spaced arrangement. At the higher heating rates the agreement between the computations and the input is somewhat worse than for the evenly spaced arrangement. The source of the error was investigated and found to be associated with the shape of the analytical curve (a third-order polynomial as in refs. 2 and 3) used to curve fit the four measured values of $c \frac{dT}{dt}$ through the wall. As shown in figure 11, there is noticeable disagreement between the third-order polynomial and the exact variation of $c \frac{dT}{dt}$ through the wall. In regard to the final answer, the important thing is, of course, not the accuracy in the shape of the polynomial but in the integrated area under the curve. For

the two sets of measurement depths shown, it is obvious that the shape of the polynomial more closely approximates that of the exact curve when measurement locations are evenly spaced. Although it is not so obvious, the integrated area for the evenly spaced arrangement is in a little better agreement than for the unevenly spaced arrangement. These results are apparent in the comparison of computed heat flux with exact input shown in figure 10. Although not shown in figure 10 or figure 11, results were determined also for measurement depths of 0.0254, 0.2032, 0.6096, and 1.524 cm. The error in the area under the polynomial became magnified even more. At 11 seconds the computed heat flux was 1220 watts/cm², which is 19.4 percent higher than the exact-input value of 1022 watts/cm² shown in figure 10. Errors due to this source become smaller relative to the heat flux for smaller physical thickness of the wall. Therefore the influence of the foregoing error on the results of references 2 and 3 was small, since the wall thickness was only 0.508 cm and the thermocouples were evenly spaced.

Computations by the integral method shown in figure 10 start after transition and end before peak heating. The reason is that in the integral program (ref. 2) the temperature-time history was expressed as a sixth-order polynomial. Sixth-order polynomials fitted to the entire temperature history from 0 to 16 seconds for each of the four depths give very poor computed heat-flux results. Therefore, care must be taken to fit the temperature history with the polynomial over regions that have no drastic changes or inflection points as occur at transition and peak heating, respectively. It may be noticed in figure 11 that the values of $c \frac{dT}{dt}$ indicated by the symbols may not fall precisely on the exact curve. The reason is that the value of $c \frac{dT}{dt}$ determined from the sixth-order polynomial, which is fitted to the temperature history, may have a slight error. Although results for lower heat flux are not shown in figure 11, calculations at 6 seconds ($q = 352$ watts/cm²) were made which show that the agreement between the third-order polynomial and the exact curve of $c \frac{dT}{dt}$ through the wall is very good (see agreement of q in fig. 10) when the gradient through the wall is small. Although a third-order polynomial fitted to $c \frac{dT}{dt}$ as a function of τ gave satisfactory results for the 0.508-cm-thick wall of references 2 and 3 (even for high heating levels), it is apparent from figure 11 that some other analytical expression may give more accurate results for thick walls with high heating. Unpublished results of an investigation of this problem by James L. Dillon of Langley Research Center indicate that a third-order exponential provides improved accuracy.

Results determined by the single-thermocouple inverse solution for a depth of 0.0254 cm and a computing interval of 0.1 second are also shown in figure 10 for

comparison. The agreement is good over the entire heating period. The input temperature history was smooth (without scatter or bias) for both methods in figure 10.

Comparison with single-thermocouple method of reference 4.- The method of reference 4 is based on the assumption that the mean value of $c \frac{dT}{dt}$ always occurs at a specific depth in the wall, namely at approximately 40 percent of the total thickness measured from the heated surface ($\frac{\tau}{\tau_t} = 0.40$). It is obvious that there is a mean value of $c \frac{dT}{dt}$ somewhere in the wall which if treated as a constant from the heated surface to the back surface (see dashed line in fig. 11) will give the same area as the integrated area under the exact curve. When $c \frac{dT}{dt}$ is treated as a constant, equation (1) is simplified and becomes

$$q = \rho \left(c \frac{dT}{dt} \right)_m \tau_t \quad (2)$$

This method was used to determine heating rates from temperatures for the case representing a reentry flight experiment with wall thickness of 1.524 cm. Results computed by this method for the 40-percent depth ($\tau = 0.6096$ cm) are in very good agreement with the exact input at the lower heating values (as shown in fig. 12), but not at the higher heating values, or in the region of maximum heating. The nondimensional location (τ/τ_t) of the mean value of $c \frac{dT}{dt}$ is not fixed; for instance, at higher heating levels the mean value of $c \frac{dT}{dt}$ progresses from the 40-percent depth toward the heated surface while the heat flux is increasing. The location is apparently dependent on material properties, heat flux, and wall thickness. As with the integral method, the accuracy of this method is also improved as the physical thickness of the wall becomes smaller, and it may be noted that good results were obtained for a 0.508-cm-thick beryllium wall, as shown in reference 4.

Also shown in figure 12 for comparison is the present single-thermocouple inverse solution for a measurement which is at the 40-percent depth. The computing interval is 0.4 second. The results are significantly better than those obtained by the method of reference 4 (eq. (2)).

Influence of Erroneous Inputs

There are several sources of error in the determination of q (some of which are obvious), namely incorrect material properties, error in location of thermocouple, biased temperature history, and scattered temperature data. The effects of these factors

were investigated for a thermocouple location 0.0254 cm below the heated surface of a 1.524-cm-thick beryllium wall (see block 2 in fig. 3). It should be noted that the errors shown in tables I to IV are due specifically to error in the parameter being considered; that is, they reflect only the effect of the parameter error and not the accuracy of the single-thermocouple inverse method.

Error in specific heat.- In order to determine the effect of error in specific heat, an assumed error in the curve for c shown in figure 2 was used in the single-thermocouple inverse solution. The effects of errors in specific heat of -2.5 percent and -5 percent are shown in table I. The percent error in the heat flux is not the same as the percent error in the specific heat, as might be expected from equation (1). Apparently, the reason is that the error in the specific heat alters the change in temperature with respect to time $\left(\frac{dT}{dt}\right)$ through the wall. In this case it appears that the secondary effect on $\frac{dT}{dt}$ tends to partially compensate the error in specific heat. The effect of this type error does not diminish as physical thickness of the wall becomes smaller.

Error in conductivity.- In order to determine the effect of error in conductivity, an assumed error in the curve for k shown in figure 2 was used in the single-thermocouple inverse solution. The effect of errors in conductivity of -2.5 percent, -5 percent, -10 percent, and +10 percent is shown in table II. The effect on the computed heat flux is as expected. However, it should be noted that with the same error in conductivity but with the measurement near the back wall, the effect on the computed heat flux would have been just the opposite in sign and that therefore there is a cross-over point somewhere within the wall where the effect of error in conductivity would be minimized. The effect of this type error diminishes as physical thickness of the wall becomes smaller.

It should be noted that when two or more thermocouple measurements are used in combination (as discussed subsequently), the effect of erroneous conductivity tends to be minimized if the thermocouple distribution nearly spans the wall thickness.

Error in measurement location.- Since the temperature and the temperature rise with respect to time $\left(\frac{dT}{dt}\right)$ vary with distance from the heated surface, it is essential that the location of the measurement be known with reasonable accuracy. Effects of location errors of 0.0254 cm and 0.0508 cm (too deep) are shown in table III; thus, temperature histories at 0.0508-cm and 0.762-cm depths were considered to be actually at a depth of 0.0254 cm. The error in the computed heat flux due to the larger location error of 0.0508 cm (see results in table for temperature history at 0.0762 cm) is approximately double that due to the smaller location error of 0.0254 cm (see results for temperature history at 0.0508 cm). The computed heat-flux errors are comparatively small even for

these large location errors (locations can be determined in practice within about ± 0.008 cm). The effect of this type error diminishes as the physical thickness becomes smaller.

Biased temperature.- Effect of temperature which is 5 percent too high is shown in table IV. It may be noted that most of the effect shown is due to the increase in rate of temperature rise $\left(\frac{dT}{dt}\right)$ associated with temperature that is too high by a constant percentage. Temperatures too high by a constant number of degrees would have had a relatively small effect on the results.

Data scatter.- All the aforementioned solutions were determined by using the smooth temperature-time histories computed by the direct thick-wall heating computer program. A solution was also obtained wherein random scatter, simulating random measurement and telemetry inaccuracies (no bias inaccuracies), was applied to the initially smooth temperature-time history. A random-number generator was used to provide statistical scatter for a 3σ value of 25° K. The scattered temperature data were smoothed by a Chebyshev curve fit of a sixth-order polynomial which was then used in the single-thermocouple inverse program to obtain a heat-flux history. The heating results were found to be in very good agreement with the exact input (within 2.5 percent), as shown in figure 13. The sixth-order polynomial curve was fitted to the temperature history over the time range of 3 to 12 seconds, since fitting the curve from a time before the abrupt change at transition to a time after maximum heating proved to be a very poor representation of the real temperature-time curve. It may be noted that this computation is actually a test of the accuracy of the sixth-order-polynomial curve-fit technique rather than a test of the single-thermocouple method per se.

SOME APPLICATIONS

Application to Flight Data

Heating-rate—time histories have been computed by the single-thermocouple inverse method for a location on each of the three beryllium heat shields (three data periods) of the Fire II reentry spacecraft (ref. 3). The thickness of each of the heat shields was 0.508 cm. The identical sixth-order polynomial curves which were fitted to the experimental temperature data in the Project Fire data analysis were used herein.

As shown in figures 14 and 15, the stagnation-point heating rates during the first and third data periods, as computed by the single-thermocouple inverse method with either of the two outermost thermocouples, are in good agreement with the data from reference 3, determined by the integral method. Since the Fire II flight data are confidential, the scale values are not given in figures 14 to 18 in order that these data can be

included herein. Figure 16 shows results from the second data period for locations on the heat shield of $\frac{s}{R} = 0.54$ and $\frac{s}{R} = 0.90$ (the comparison was made at these locations rather than at the stagnation point because of failure of thermocouples at the stagnation point). Because of the noticeable disagreement between results from the two outermost thermocouples at both s/R locations, single-thermocouple-method results were computed by using each of the four thermocouples at these two stations. The integral-method data of reference 3 is roughly the average of the results from the four individual thermocouples. The source of the difference between results from the individual thermocouples during this data period has not been determined, although certain possibilities have been considered. Temperature gradients through the wall at the beginning of the heating period, which were initially suspected as possible contributing factors, were studied and found to damp out quickly after the heating commenced. Also, the flight temperature measurements at different radial locations indicate that lateral conduction was negligible and could not be the source of the discrepancies. It may be noted, however, that the temperature rise was much more rapid during the second data period than during the first or third period, as shown in figure 17. This rapid rise results in fewer points per unit temperature rise and thus less accuracy in defining the temperature curves. For this reason more variation between the individual-thermocouple results might be expected during the second data period than during the other data periods.

It may be noted that a machine technique has been developed to utilize multiple-thermocouple data with the basic, single-thermocouple inverse method. The same thick-wall, finite-difference computation program is used, but instead of finding the heating rate q that produces the one measured temperature-time history, the criterion for the desired q is that the sum of the temperature errors at the four measurement depths (or as many as are available) be zero. That is, the sum of the computed temperatures at the measurement depths must equal the sum of the experimental temperatures. This method is believed to be an improvement over averaging the values of q obtained from individual measurements containing experimental inaccuracies, since it effectively gives more weight to the more sensitive measurements (i.e., those thermocouples nearer the heated surface). The heating rates computed by this method in the second data period for the location $\frac{s}{R} = 0.90$ are compared in figure 18 with the integral-method results of reference 3. The two sets of results are within 2 or 3 percent of each other.

Other Possible Applications

It is believed that the single-thermocouple inverse method could be used to account for gas (as a coolant) being blown through a porous wall. This application would require that the heat-balance equations (shown in the appendix) be extended to include the effects of the mass-flow rate and physical properties of the gas.

The method could also conceivably be used in other applications, such as determining the conductivity (or specific heat) of a material by iterating, for example, an assumed value of conductivity until temperature measurements at two or more different depths are satisfied.

CONCLUDING REMARKS

A method for determining heating rates from a single temperature-time history within a thermally thick wall has been developed. This method accounts for variable thermal properties, can be used for a composite wall, and can account for surface-radiation effects in the analytical computations if so desired. The method has been analyzed for a 1.524-cm-thick beryllium wall and the following points noted:

1. The accuracy depends primarily on the thermal depth of the measurement point, and ranges from good to excellent for a number of practical cases, with best results occurring for temperature measurements nearest the heated surface in conjunction with a small computing interval.

2. If the measurement is sufficiently near the heated surface, the method can detect sudden changes in the slope of heat flux such as are experienced when boundary-layer flow becomes transitional or when heating-rate history oscillates.

3. A comparison with an integral method and with another single-thermocouple method shows that the present method is more accurate for the heat-flux histories and the thermal model considered herein.

4. The method is not restricted to data from only one measurement, but can utilize any number of measurements and therefore all available data for any given station.

Langley Research Center,

National Aeronautics and Space Administration,

Langley Station, Hampton, Va., May 14, 1968,

711-02-09-01-23.

APPENDIX

THICK-WALL HEAT-BALANCE EQUATIONS

The basic thick-wall heating computer program utilizes a backwards finite-difference computing technique. The finite-difference equations are solved simultaneously by the Gauss-Seidel method. The heat-balance equations used in the program for one-dimensional heat flow are (for a wall divided into four blocks) as follows:

$$\begin{array}{c}
 \text{Heat in} \\
 \downarrow \\
 qA
 \end{array}
 -
 \begin{array}{c}
 \text{Heat radiated out} \\
 \downarrow \\
 A\epsilon\sigma(T_1')^4
 \end{array}
 -
 \begin{array}{c}
 \text{Heat stored} \\
 \downarrow \\
 A\Delta\tau_1\rho c \frac{T_1 - T_1'}{\Delta t}
 \end{array}
 -
 \begin{array}{c}
 \text{Heat conducted out} \\
 \downarrow \\
 2A \frac{T_1 - T_2}{\left(\frac{\Delta\tau}{k}\right)_1 + \left(\frac{\Delta\tau}{k}\right)_2}
 \end{array}
 = 0 \quad (\text{A1})$$

$$\begin{array}{c}
 \text{Heat conducted in} \\
 \downarrow \\
 2A \frac{T_1 - T_2}{\left(\frac{\Delta\tau}{k}\right)_1 + \left(\frac{\Delta\tau}{k}\right)_2}
 \end{array}
 -
 \begin{array}{c}
 \text{Heat stored} \\
 \downarrow \\
 A\Delta\tau_2\rho c \frac{T_2 - T_2'}{\Delta t}
 \end{array}
 -
 \begin{array}{c}
 \text{Heat conducted out} \\
 \downarrow \\
 2A \frac{T_2 - T_3}{\left(\frac{\Delta\tau}{k}\right)_2 + \left(\frac{\Delta\tau}{k}\right)_3}
 \end{array}
 = 0 \quad (\text{A2})$$

$$\begin{array}{c}
 \text{Heat conducted in} \\
 \downarrow \\
 2A \frac{T_2 - T_3}{\left(\frac{\Delta\tau}{k}\right)_2 + \left(\frac{\Delta\tau}{k}\right)_3}
 \end{array}
 -
 \begin{array}{c}
 \text{Heat stored} \\
 \downarrow \\
 A\Delta\tau_3\rho c \frac{T_3 - T_3'}{\Delta t}
 \end{array}
 -
 \begin{array}{c}
 \text{Heat conducted out} \\
 \downarrow \\
 2A \frac{T_3 - T_4}{\left(\frac{\Delta\tau}{k}\right)_3 + \left(\frac{\Delta\tau}{k}\right)_4}
 \end{array}
 = 0 \quad (\text{A3})$$

$$\begin{array}{c}
 \text{Heat conducted in} \\
 \downarrow \\
 2A \frac{T_3 - T_4}{\left(\frac{\Delta\tau}{k}\right)_3 + \left(\frac{\Delta\tau}{k}\right)_4}
 \end{array}
 -
 \begin{array}{c}
 \text{Heat stored} \\
 \downarrow \\
 A\Delta\tau_4\rho c \frac{T_4 - T_4'}{\Delta t}
 \end{array}
 -
 \begin{array}{c}
 \text{Heat radiated out} \\
 \downarrow \\
 A\epsilon\sigma(T_4')^4
 \end{array}
 = 0 \quad (\text{A4})$$

APPENDIX

In these equations T' is the temperature at the beginning of the time interval and T is the temperature at the end of the time interval. Thermal properties (c , k , and ϵ) are based on T' .

In the basic thick-wall program operation, q is known and the unknowns are T_1 , T_2 , T_3 , and T_4 . Therefore, a unique solution exists for the unknown temperatures since the number of independent equations provided and the number of unknowns are the same. In the single-thermocouple inverse method as described in the section "Procedure and Mechanics of New Method," an assumed value of q is used in order to solve for the temperature at each block. If, however, the temperature history is known at one block, it is not necessary to solve for temperature at that location, and thus q could be considered as one of the unknowns without increasing the number of unknowns over the number of equations. Then q could be solved for directly without going through an iteration on an assumed q . A program utilizing a matrix solution, which will solve for q directly, has been written. This system is solved by a library subroutine which solves the matrix equation $\bar{A}X = \bar{B}$ (where \bar{A} is a square coefficient matrix and \bar{B} is a column vector). The heating rate is evaluated by a subroutine in place of the known temperature.

REFERENCES

1. Hill, P. R.: A Method of Computing the Transient Temperature of Thick Walls From Arbitrary Variation of Adiabatic-Wall Temperature and Heat-Transfer Coefficient. NACA Rep. 1372, 1958. (Supersedes NACA TN 4105.)
2. Cornette, Elden S.: Forebody Temperatures and Total Heating Rates Measured During Project Fire I Reentry at 38 000 Feet Per Second. NASA TM X-1120, 1965.
3. Cornette, Elden S.: Forebody Temperatures and Calorimeter Heating Rates Measured During Project Fire II Reentry at 11.35 Kilometers Per Second. NASA TM X-1305, 1966.
4. McDonough, John F.; and Youngbluth, Otto, Jr.: A Simple Method for Determining High Heat Rates by Using Slug Calorimeters. NASA TM X-1408, 1967.
5. Stroud, C. W.: A Numerical Method for Determining Heating Rates From Thick-Calorimeter Data. NASA TN D-3846, 1967.
6. Gaumer, G. R.; Parks, D. L.; and Kipp, H. W.: ASSET. Volume XIV - Heat Flux Calculation Procedures. Tech. Rep. AFFDL-TR-65-31, vol. XIV, U.S. Air Force, Apr. 1966. (Available from DDC as AD 480814.)
7. Stolz, G., Jr.: Numerical Solutions to an Inverse Problem of Heat Conduction for Simple Shapes. Trans. ASME, Ser. C: J. Heat Transfer, vol. 82, no. 1, Feb. 1960, pp. 20-26.
8. Beck, James V.: Calculation of Surface Heat Flux From an Internal-Temperature History. Paper No. 62-HT-46, Amer. Soc. Mech. Eng., 1962.
9. Frank, Irving: An Application of Least Squares Method to the Solution of the Inverse Problem of Heat Conduction. Trans. ASME, Ser. C: J. Heat Transfer (Tech. Briefs), vol. 85, no. 4, Nov. 1963, pp. 378-379.
10. Sparrow, E. M.; Haji-Sheikh, A.; and Lundgren, T. S.: The Inverse Problem in Transient Heat Conduction. Trans. ASME, Ser. E: J. Appl. Mech., vol. 31, no. 3, Sept. 1964, pp. 369-375.
11. Burggraf, O. R.: An Exact Solution of the Inverse Problem in Heat Conduction Theory and Applications. Trans. ASME, Ser. C: J. Heat Transfer, vol. 86, no. 3, Aug. 1964, pp. 373-382.
12. Powell, Walter B.; and Price, Theodore W.: A Method for the Determination of Local Heat Flux From Transient Temperature Measurements. ISA Trans., vol. 3, no. 3, July 1964, pp. 246-254.

13. Howard, Floyd G.: Heat Transfer on Unswept and 38° Swept Cylindrically Blunted Wedge Fins in Free Flight to Mach Number 4.11. NASA TN D-2386, 1964.

TABLE I.- EFFECT OF ERROR IN SPECIFIC HEAT (c) ON
INVERSE HEAT-FLUX COMPUTATIONS

Time, sec	q_2 , watts/cm ²	q_E , watts/cm ²	$q_E - q_2$, watts/cm ²	Percent error
Error in specific heat of -2.5 percent				
1.1	26.39	26.23	-0.16	-0.60
2.1	29.59	29.17	-.42	-1.42
3.1	65.94	64.90	-1.04	-1.57
4.1	170.19	167.67	-2.52	-1.48
5.1	276.17	271.93	-4.24	-1.53
6.1	363.92	358.06	-5.86	-1.61
7.1	471.32	463.56	-7.76	-1.65
8.1	595.30	585.44	-9.86	-1.66
9.1	743.02	730.77	-12.25	-1.65
10.1	891.44	876.89	-14.55	-1.63
11.1	1043.89	1027.07	-16.82	-1.61
Error in specific heat of -5 percent				
1.1	26.39	26.06	-0.33	-1.25
2.1	29.59	28.74	-.85	-2.88
3.1	65.94	63.86	-2.08	-3.15
4.1	170.19	165.11	-5.08	-2.99
5.1	276.17	267.64	-8.53	-3.09
6.1	363.92	352.11	-11.81	-3.24
7.1	471.32	455.69	-15.63	-3.32
8.1	595.30	575.43	-19.87	-3.34
9.1	743.02	718.36	-24.66	-3.32
10.1	891.44	862.15	-29.29	-3.29
11.1	1043.89	1010.05	-33.84	-3.24

TABLE II.- EFFECT OF ERROR IN CONDUCTIVITY (k) ON
INVERSE HEAT-FLUX COMPUTATIONS

Time, sec	q_2 , watts/cm ²	q_E , watts/cm ²	$q_E - q_2$, watts/cm ²	Percent error
Conductivity error of -2.5 percent				
1.1	26.39	25.89	-0.50	-1.89
2.1	29.59	29.26	-.33	-1.11
3.1	65.94	65.30	-.64	-.96
4.1	170.19	168.42	-1.77	-1.04
5.1	276.17	273.42	-2.75	-.99
6.1	363.92	360.58	-3.34	-.92
7.1	471.32	467.19	-4.13	-.88
8.1	595.30	590.14	-5.16	-.87
9.1	743.02	736.54	-6.48	-.87
10.1	891.44	883.53	-7.91	-.89
11.1	1043.89	1034.39	-9.50	-.91
Conductivity error of -5 percent				
1.1	26.39	25.39	-1.00	-3.78
2.1	29.59	28.93	-.66	-2.22
3.1	65.94	64.64	-1.30	-1.98
4.1	170.19	166.61	-3.58	-2.10
5.1	276.17	270.62	-5.55	-2.01
6.1	363.92	357.15	-6.77	-1.86
7.1	471.32	462.95	-8.37	-1.78
8.1	595.30	584.85	-10.45	-1.76
9.1	743.02	729.89	-13.13	-1.77
10.1	891.44	875.43	-16.01	-1.80
11.1	1043.89	1024.71	-19.18	-1.84

TABLE II.- EFFECT OF ERROR IN CONDUCTIVITY (k) ON
 INVERSE HEAT-FLUX COMPUTATIONS - Concluded

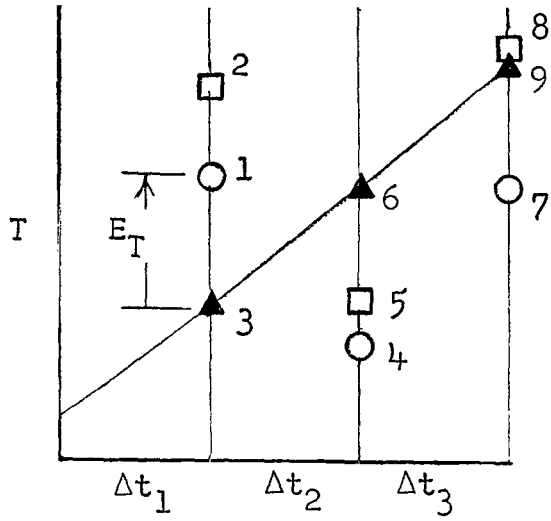
Time, sec	q_2 , watts/cm ²	q_E , watts/cm ²	$q_E - q_2$, watts/cm ²	Percent error
Conductivity error of -10 percent				
1.1	26.39	24.50	-1.89	-7.16
2.1	29.59	29.54	-.05	-.17
3.1	65.94	57.50	-8.44	-12.80
4.1	170.19	167.24	-2.94	-1.73
5.1	276.17	263.98	-12.19	-4.41
6.1	363.92	353.82	-10.10	-2.78
7.1	471.32	450.67	-20.65	-4.38
8.1	595.30	579.75	-15.55	-2.61
9.1	743.02	707.58	-35.44	-4.77
10.1	891.44	867.12	-24.32	-2.73
11.1	1043.89	998.93	-44.96	-4.31
Conductivity error of +10 percent				
1.1	26.39	28.50	+2.11	+8.00
2.1	29.59	32.26	+2.67	+9.02
3.1	65.94	61.97	-3.97	-6.02
4.1	170.19	181.72	+11.53	+6.77
5.1	276.17	285.72	+9.55	+3.46
6.1	363.92	380.74	+16.82	+4.62
7.1	471.32	483.39	+12.07	+2.56
8.1	595.30	621.70	+26.40	+4.43
9.1	743.02	759.08	+16.06	+2.16
10.1	891.44	930.73	+39.26	+4.40
11.1	1043.89	1073.62	+29.73	+2.85

TABLE III.- EFFECT OF ERROR IN THERMOCOUPLE LOCATION
ON INVERSE HEAT-FLUX COMPUTATIONS

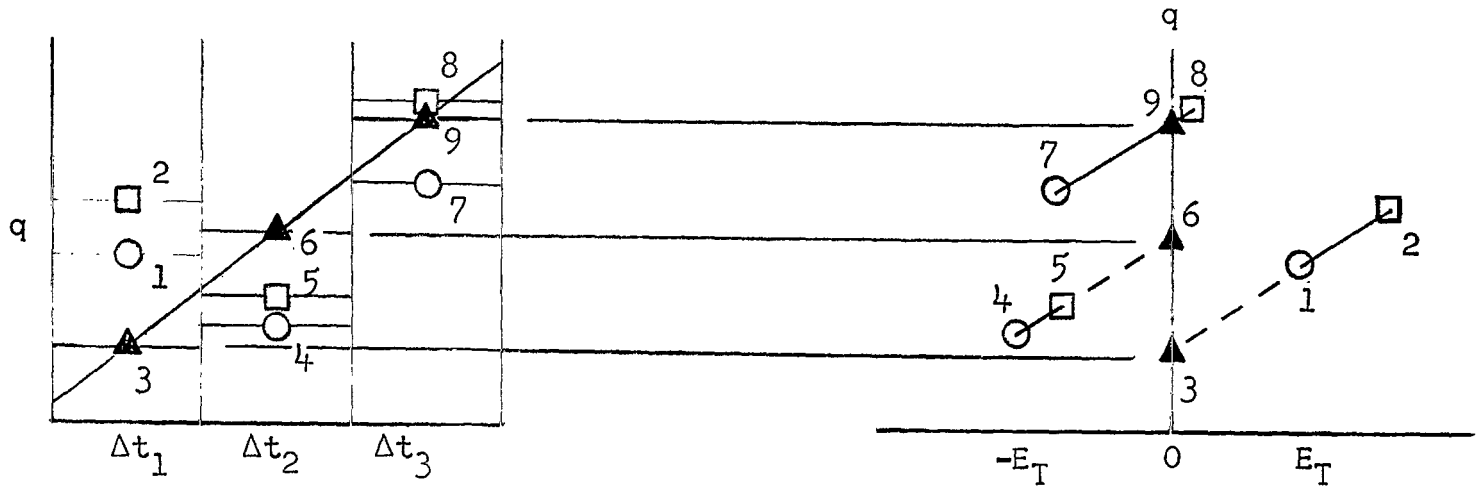
Time, sec	q_2 , watts/cm ²	q_E , watts/cm ²	$q_E - q_2$, watts/cm ²	Percent error
Temperature history at 0.0508 cm assumed to be at 0.0254 cm (Error of 0.0254 cm)				
1.1	26.39	24.14	-2.25	-8.52
2.1	29.59	28.97	-.62	-2.07
3.1	65.94	63.26	-2.68	-4.06
4.1	170.19	164.46	-5.73	-3.37
5.1	276.17	268.73	-7.44	-2.69
6.1	363.92	354.78	-9.14	-2.51
7.1	471.32	459.70	-11.62	-2.47
8.1	595.30	579.29	-16.01	-2.69
9.1	743.02	720.41	-22.61	-3.04
10.1	891.44	860.61	-30.83	-3.46
11.1	1043.89	1001.08	-42.81	-4.10
Temperature history at 0.0762 cm assumed to be at 0.0254 cm (Error of 0.0508 cm)				
1.1	26.39	21.94	-4.45	-16.86
2.1	29.59	28.36	-1.23	-4.14
3.1	65.94	60.73	-5.21	-7.90
4.1	170.19	158.89	-11.30	-6.64
5.1	276.17	261.52	-14.65	-5.31
6.1	363.92	346.00	-17.92	-4.92
7.1	471.32	448.55	-22.77	-4.83
8.1	595.30	564.06	-31.24	-5.25
9.1	743.02	699.29	-43.73	-5.89
10.1	891.44	832.15	-59.29	-6.65
11.1	1043.89	963.44	-80.45	-7.71

TABLE IV.- EFFECT OF BIASED TEMPERATURE ON
INVERSE HEAT-FLUX COMPUTATIONS

Time, sec	q_2 , watts/cm ²	q_E , watts/cm ²	$q_E - q_2$, watts/cm ²	Percent error
Temperature error of +5 percent				
1.1	26.39	27.63	+1.24	+4.73
2.1	29.59	31.41	+5.34	+6.14
3.1	65.94	70.20	+4.26	+6.47
4.1	170.19	180.37	+10.18	+5.98
5.1	276.17	292.29	+16.12	+5.84
6.1	363.92	384.07	+20.15	+5.54
7.1	471.32	495.45	+24.13	+5.12
8.1	595.30	622.55	+27.25	+4.58
9.1	743.02	773.65	+30.63	+4.12
10.1	891.44	923.52	+32.08	+3.60
11.1	1043.89	1078.38	+34.49	+3.30



(a) Temperature as function of time.



(b) Heat flux as function of time.

(c) Heat flux as function of temperature error.

Figure 1.- Mechanics and procedure of single-thermocouple inverse solution.

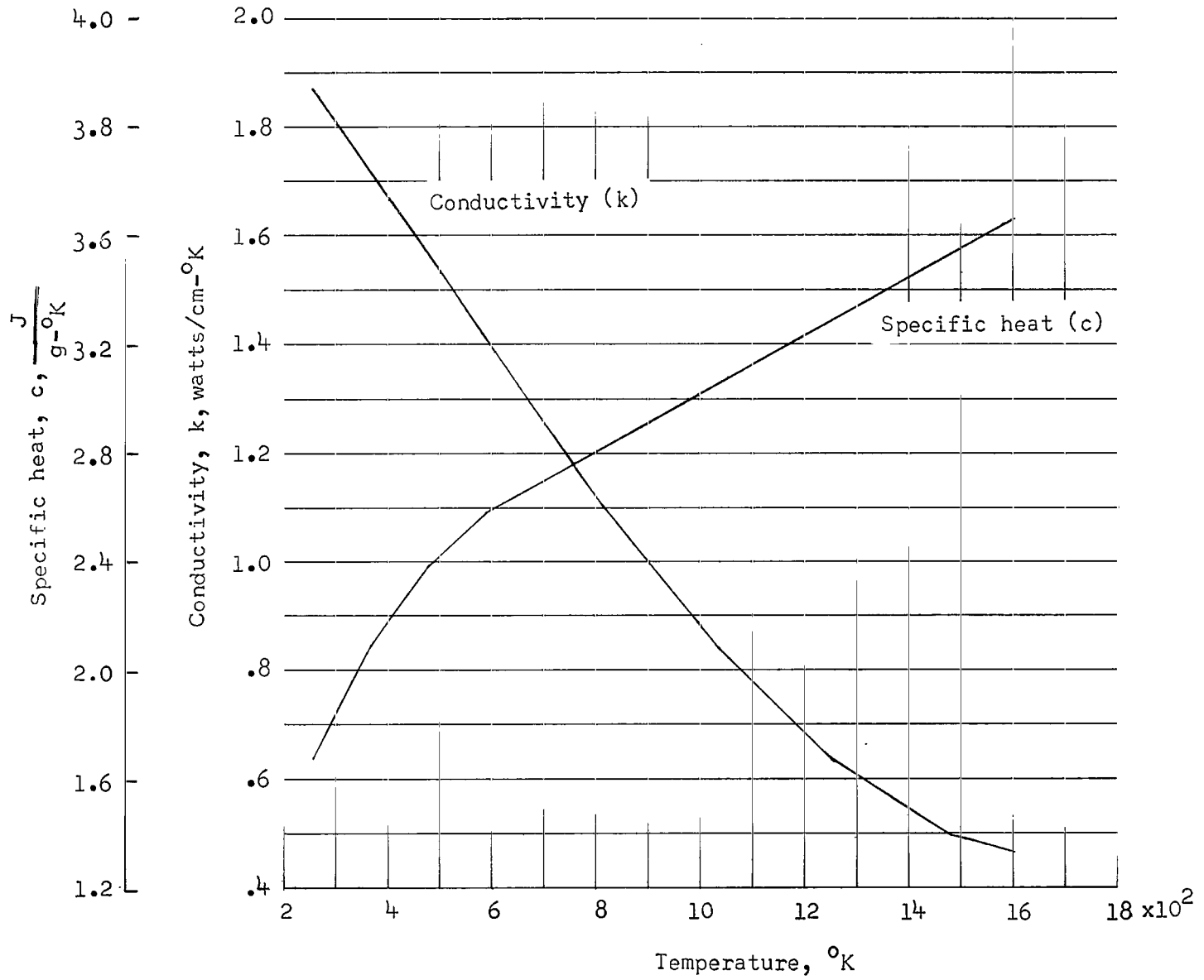


Figure 2.- Thermal properties for beryllium.

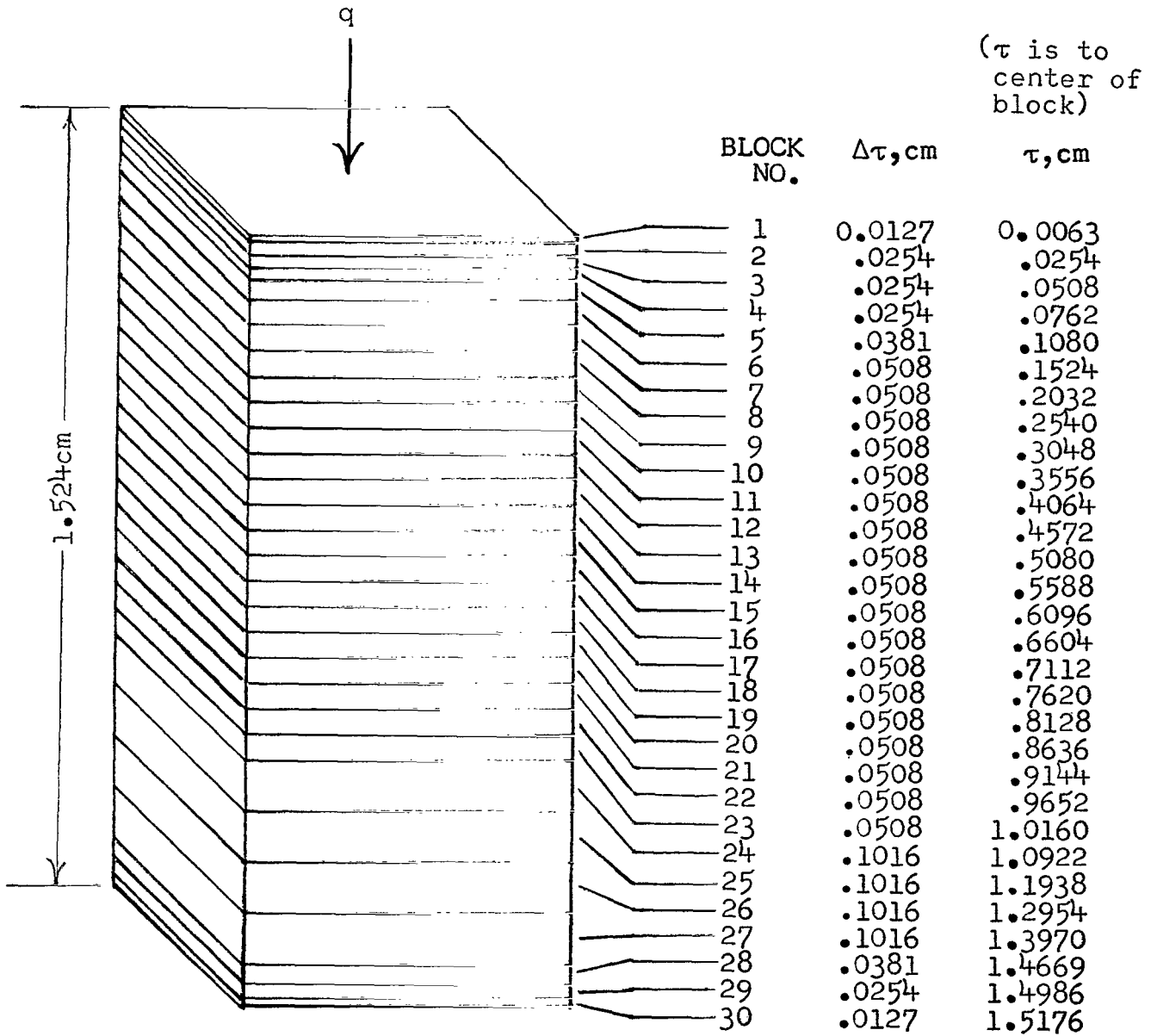


Figure 3.- Mathematical model of 1.524-cm-thick beryllium wall.

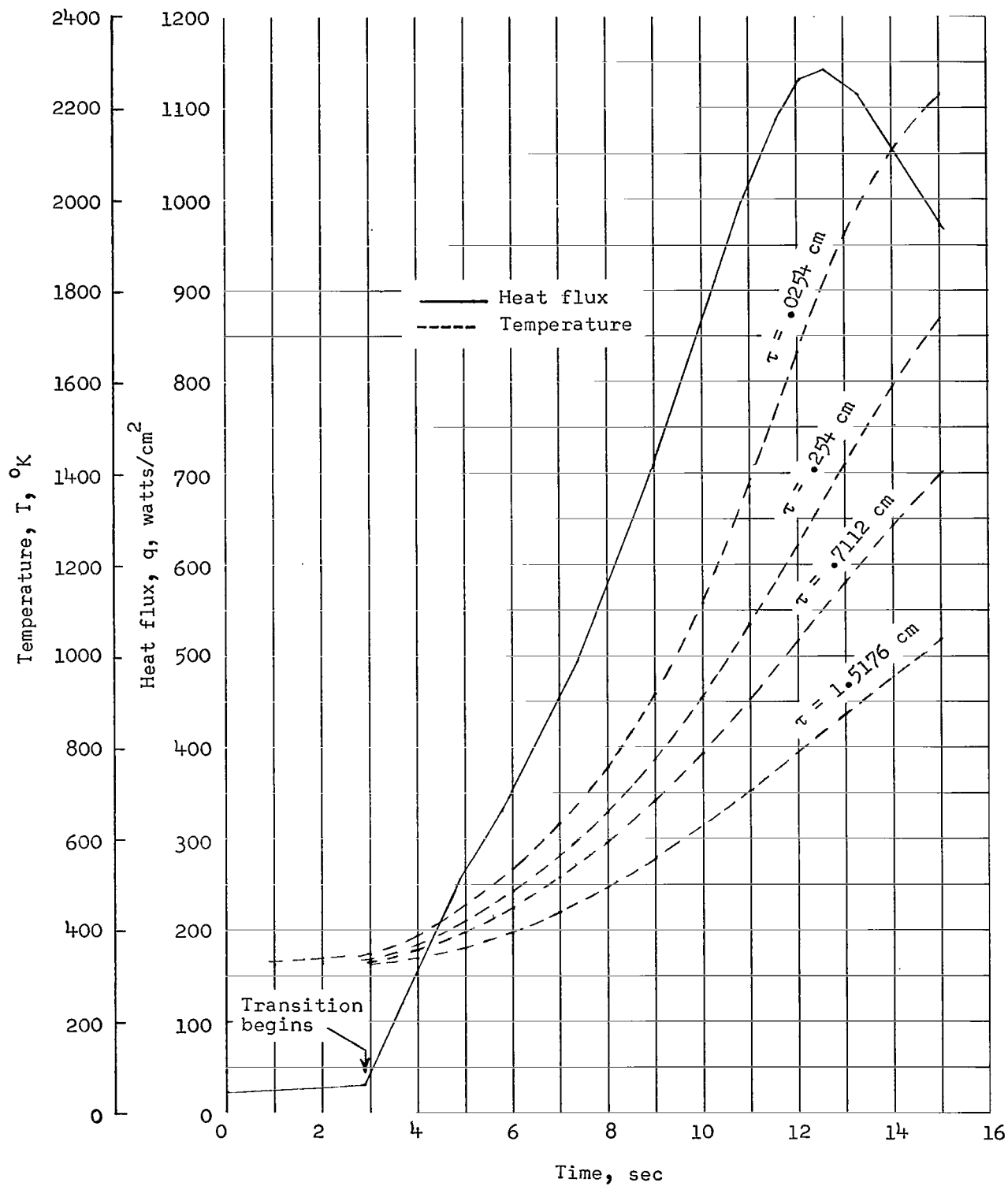
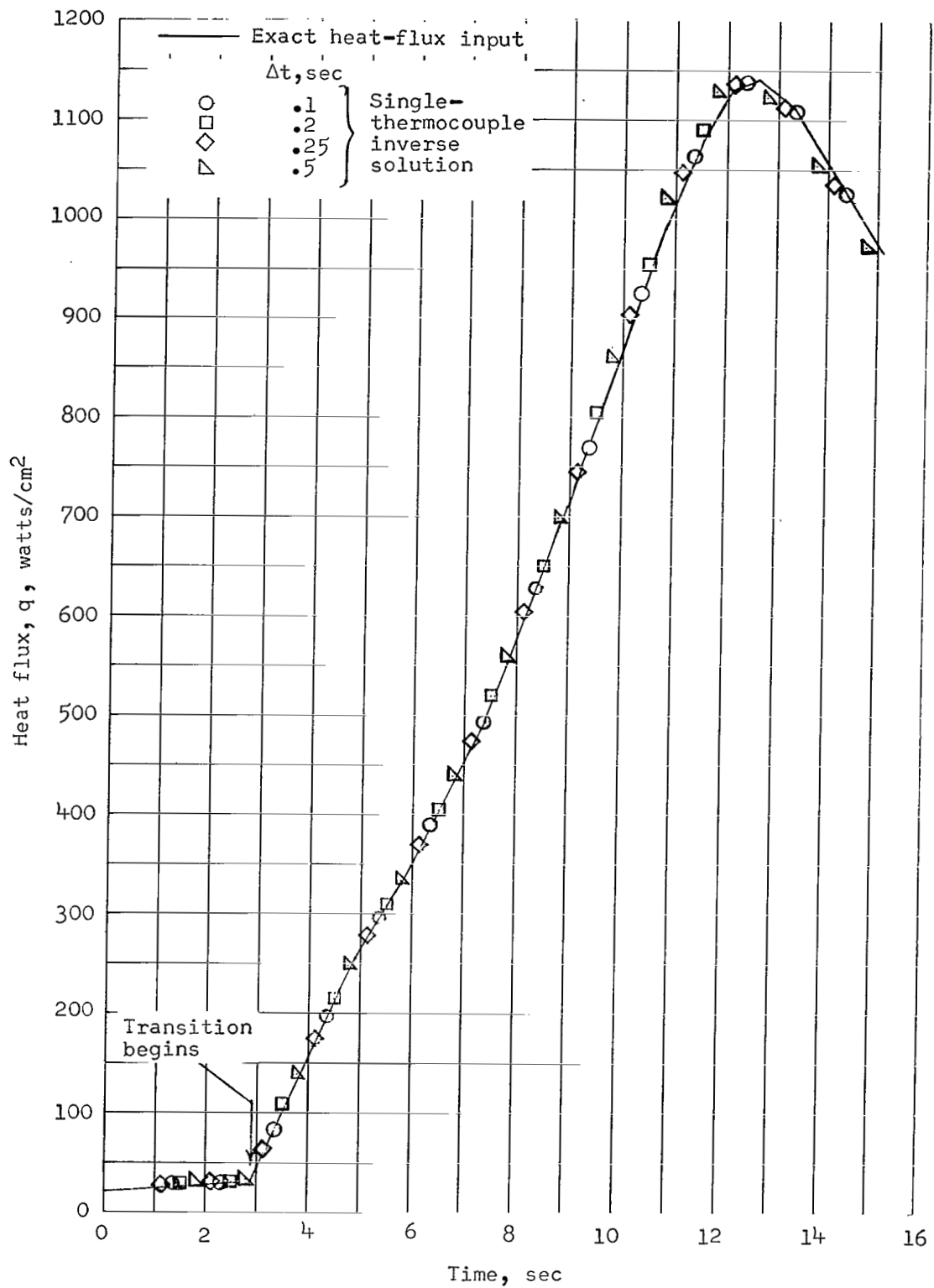
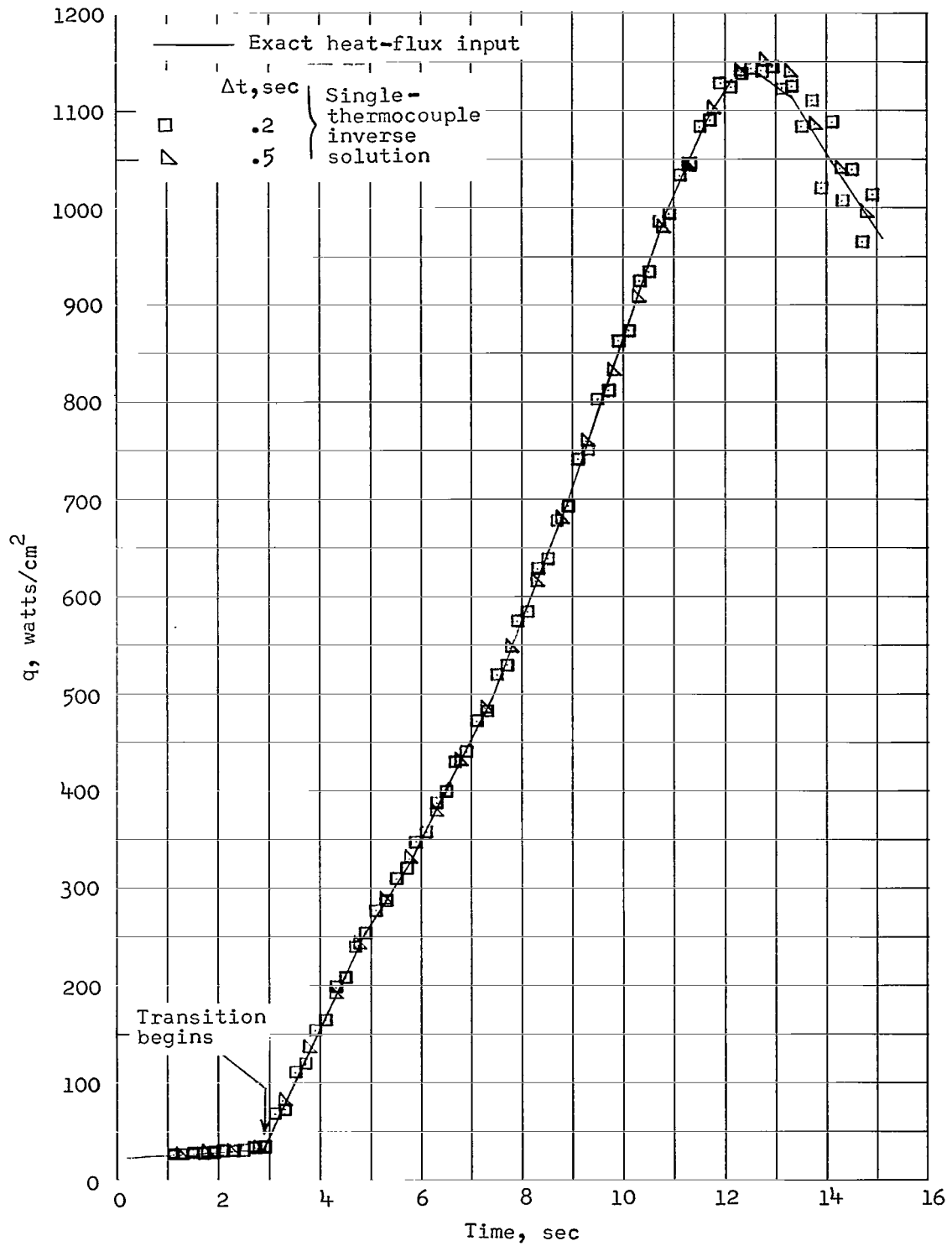


Figure 4.- Heat-flux history and associated temperature history for different depths in 1.524-cm-thick wall.



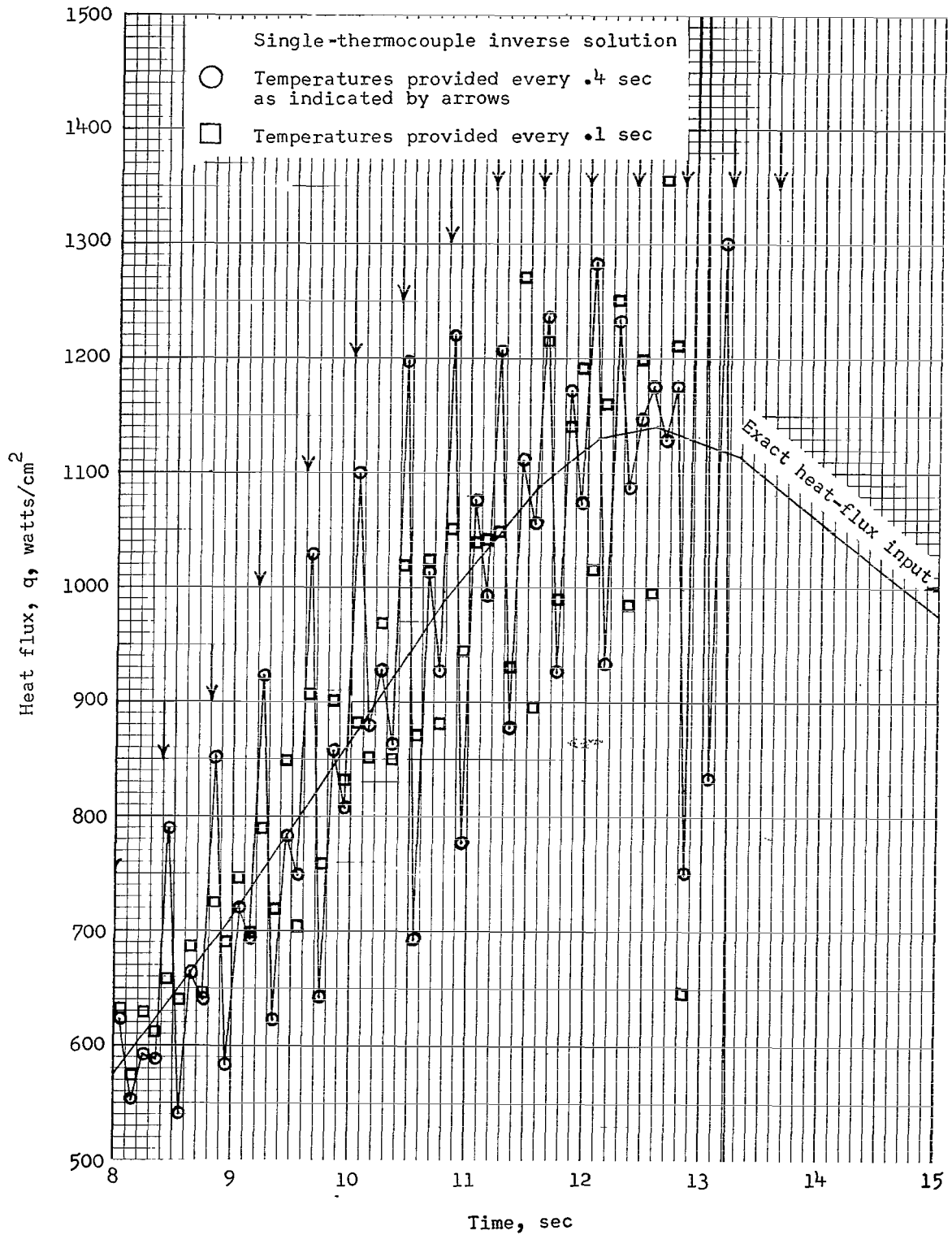
(a) Input temperature at $\tau = 0.0254$ cm.

Figure 5.- Effect of computing time interval Δt on computations by the single-thermocouple inverse method, with the exact input for a smoothly changing heat flux shown for comparison. $\tau_t = 1.524$ cm.



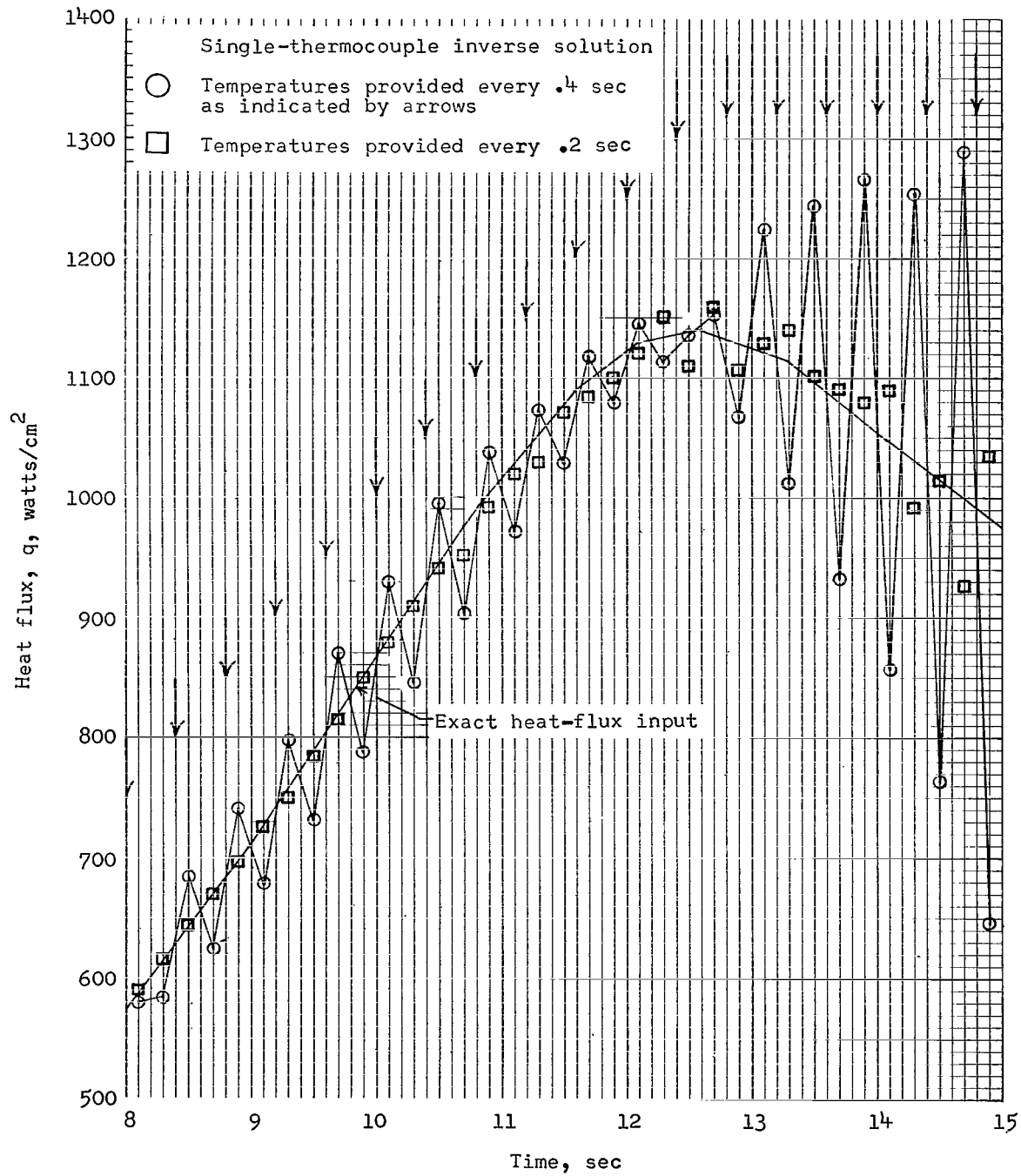
(b) Input temperature at $\tau = 0.2540 \text{ cm}$.

Figure 5.- Concluded.



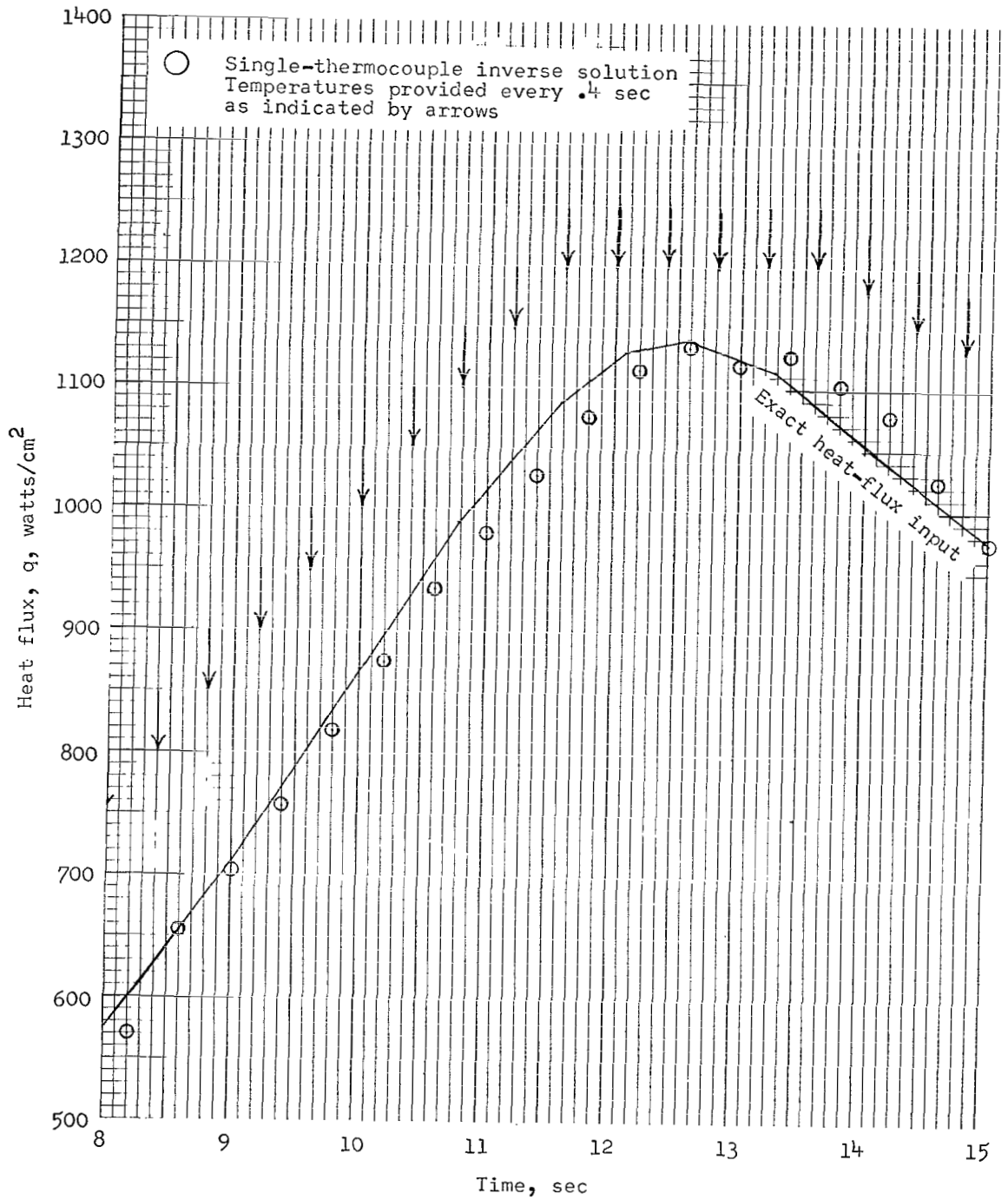
(a) $\Delta t = 0.1$ second.

Figure 6.- Influence of computing interval and temperature-input frequency on oscillations of heat flux computed by the single-thermocouple inverse method, with the exact heat-flux input shown for comparison. $\tau = 0.6096$ cm; $\tau_t = 1.524$ cm.



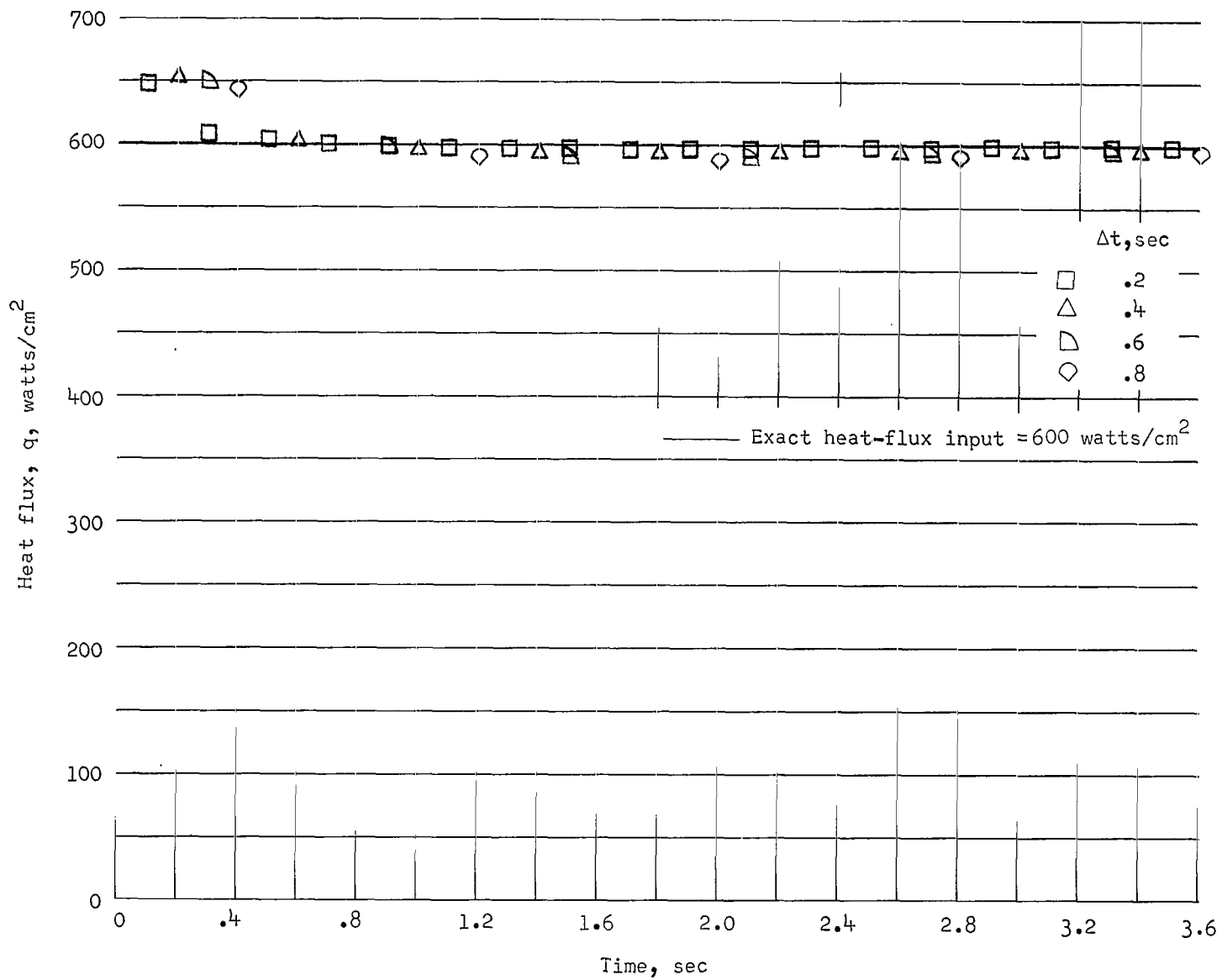
(b) $\Delta t = 0.2$ second.

Figure 6.- Continued.



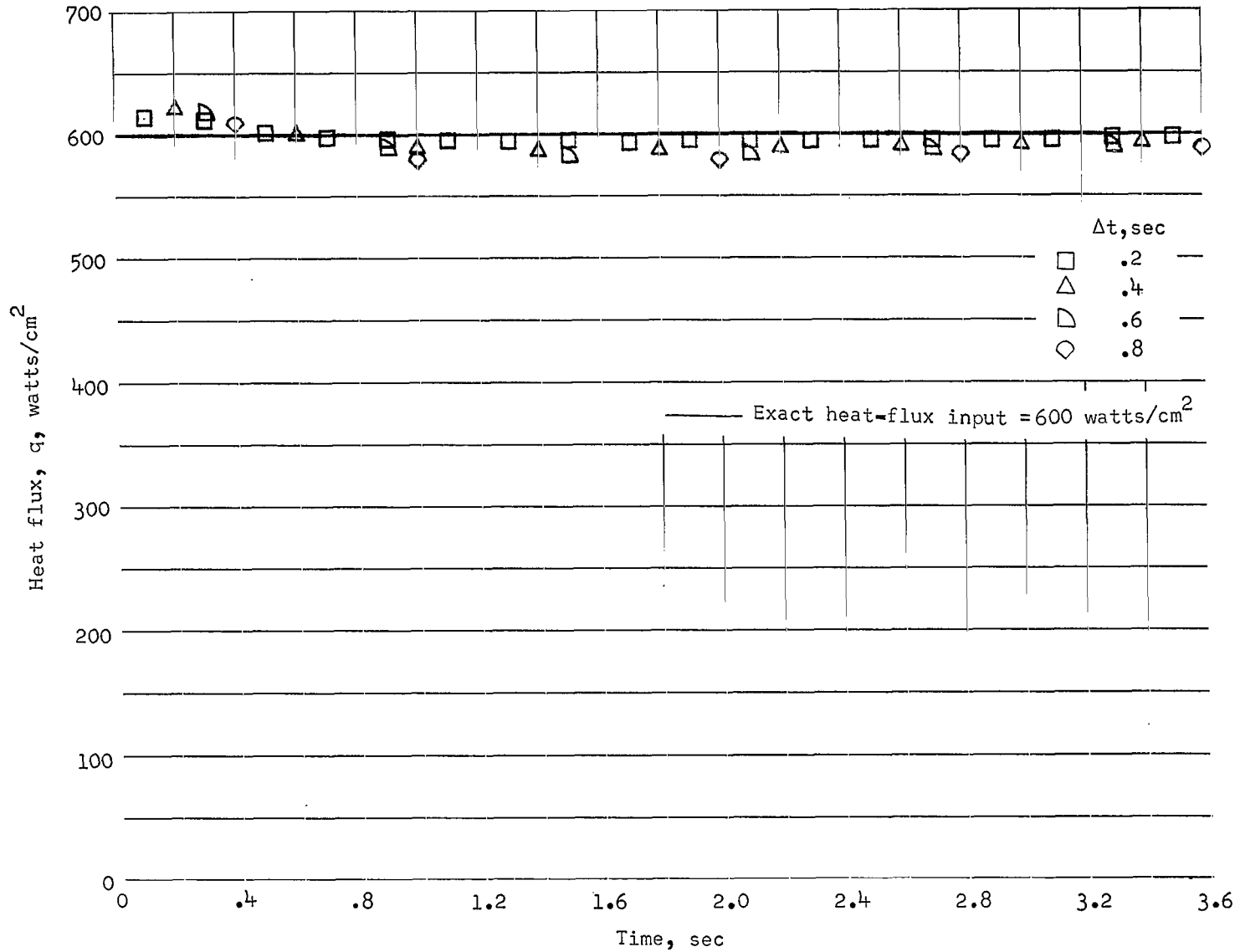
(c) $\Delta t = 0.4$ second.

Figure 6.- Concluded.



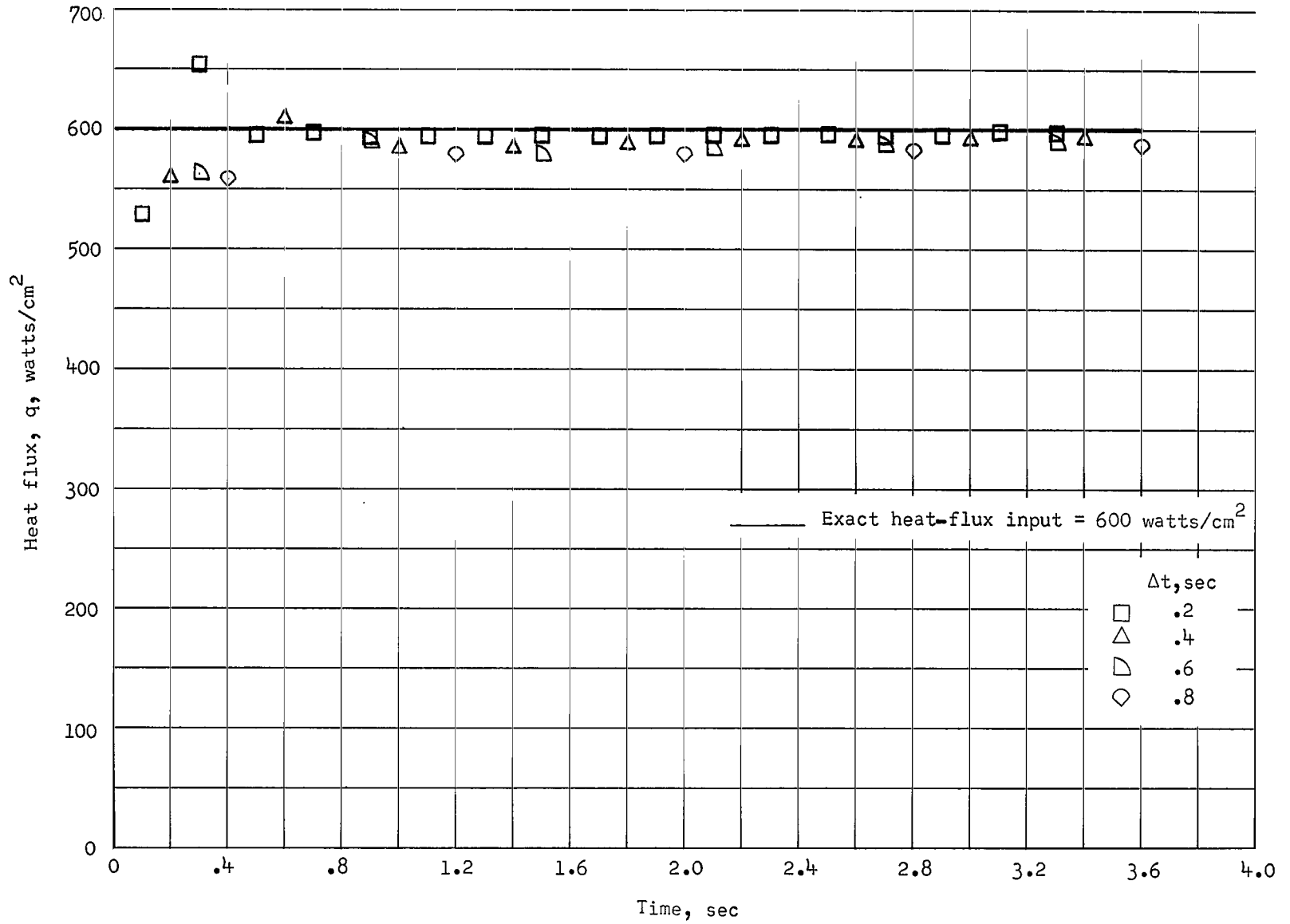
(a) Input temperature at $\tau = 0.0254$ cm.

Figure 7.- Comparison of constant and exact heat-flux inputs to 1.524-cm beryllium wall.



(b) Input temperature at $\tau = 0.2540$ cm.

Figure 7.- Continued.



(c) Input temperature at $\tau = 0.5080$ cm.

Figure 7.- Concluded.

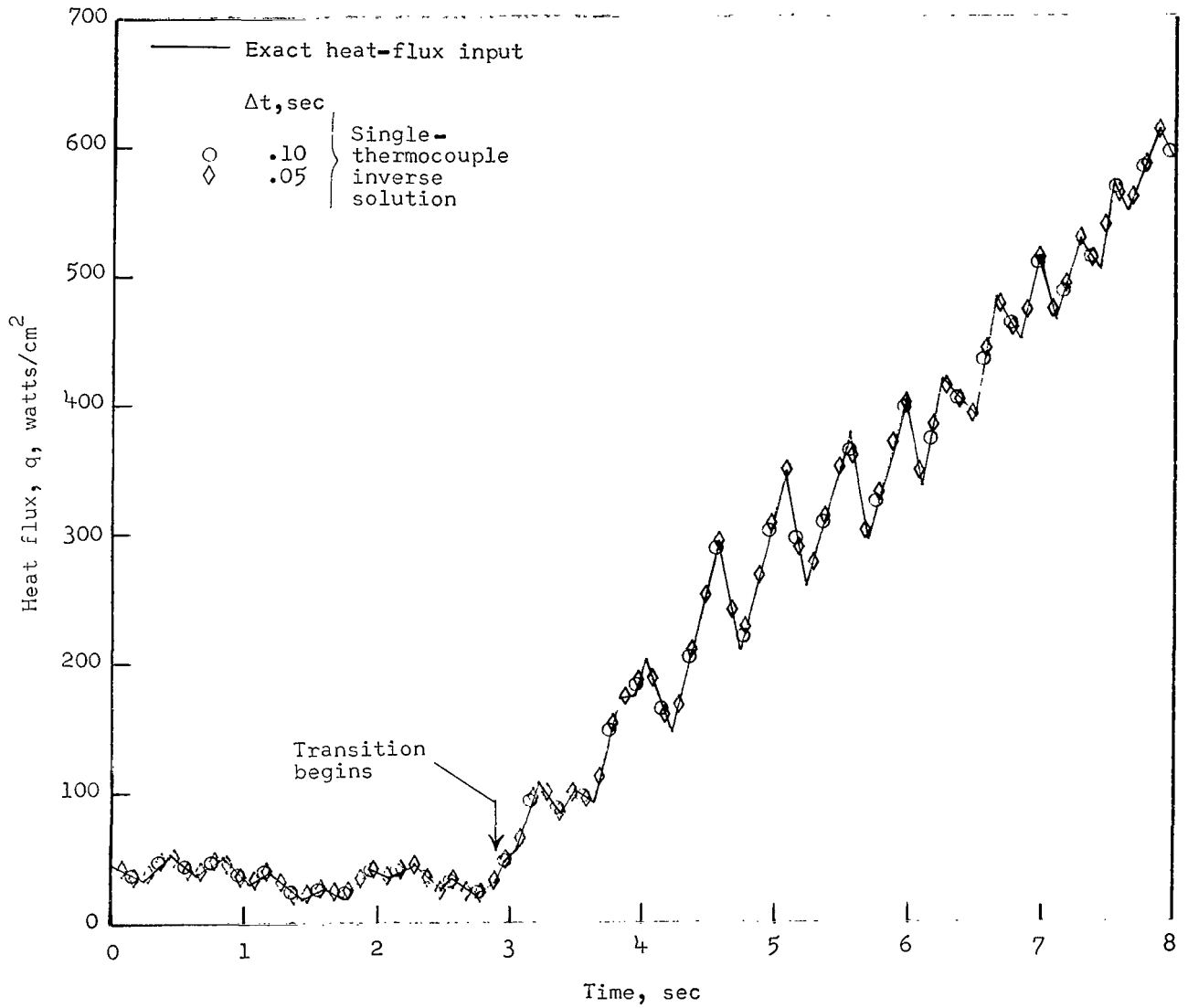


Figure 8.- Comparison of single-thermocouple inverse solutions with exact input for an oscillating heat flux. $\tau = 0.0254$ cm.

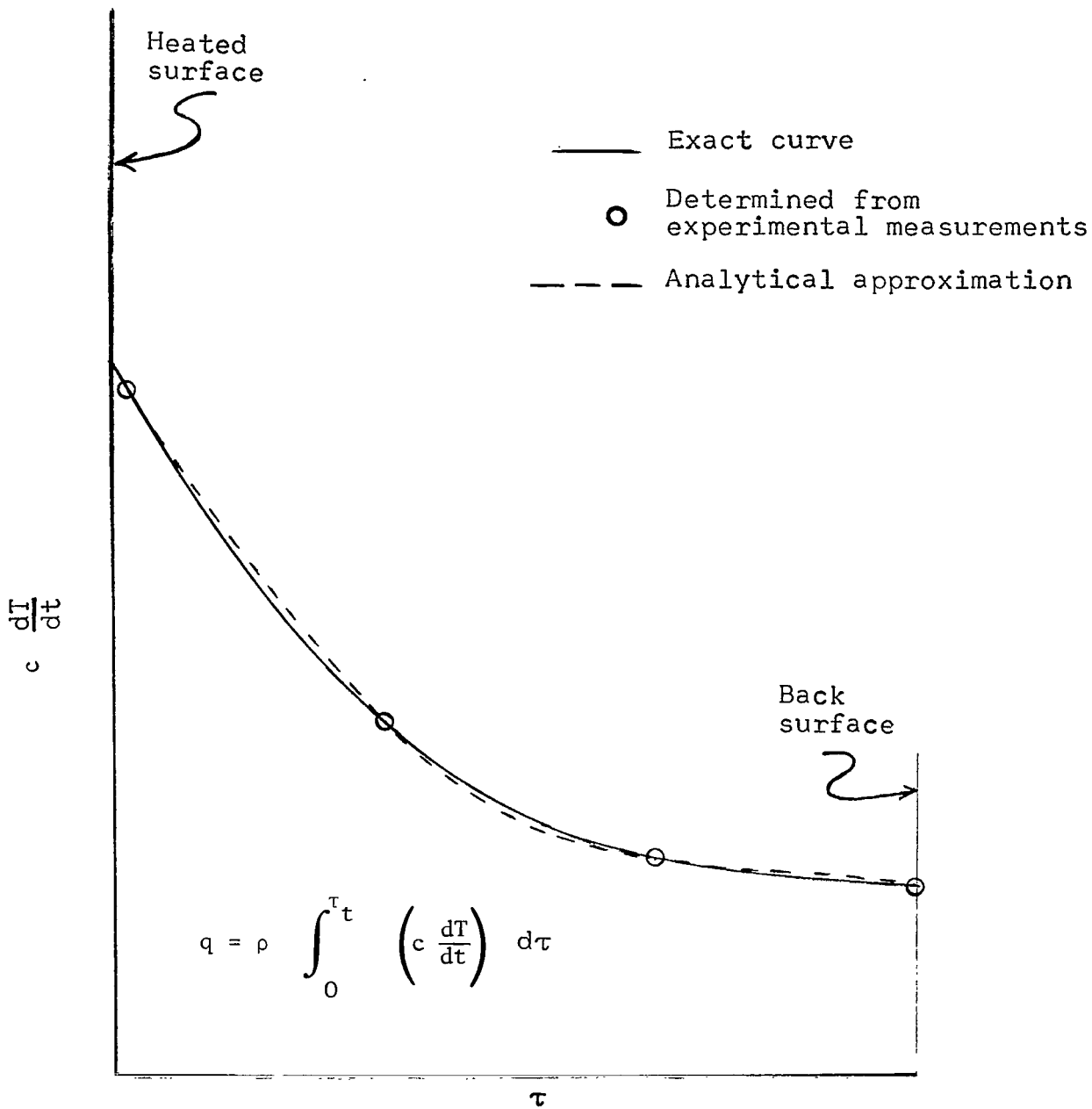


Figure 9.- Illustration of solution by method of reference 2.

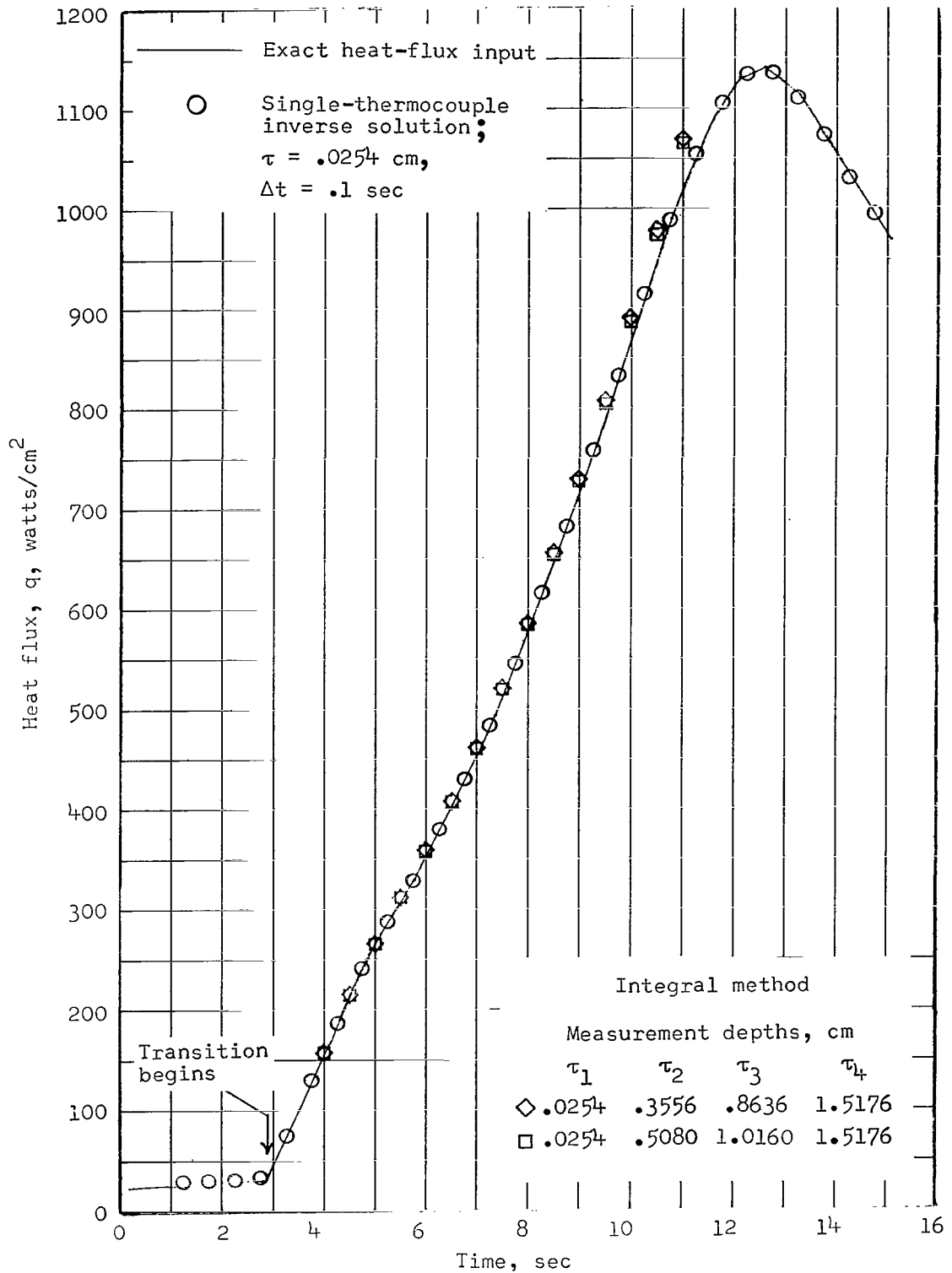


Figure 10.- Single-thermocouple inverse solutions and results obtained by the integral method of reference 2, with the exact heat-flux input shown for comparison. $\tau_4 = 1.524$ cm.

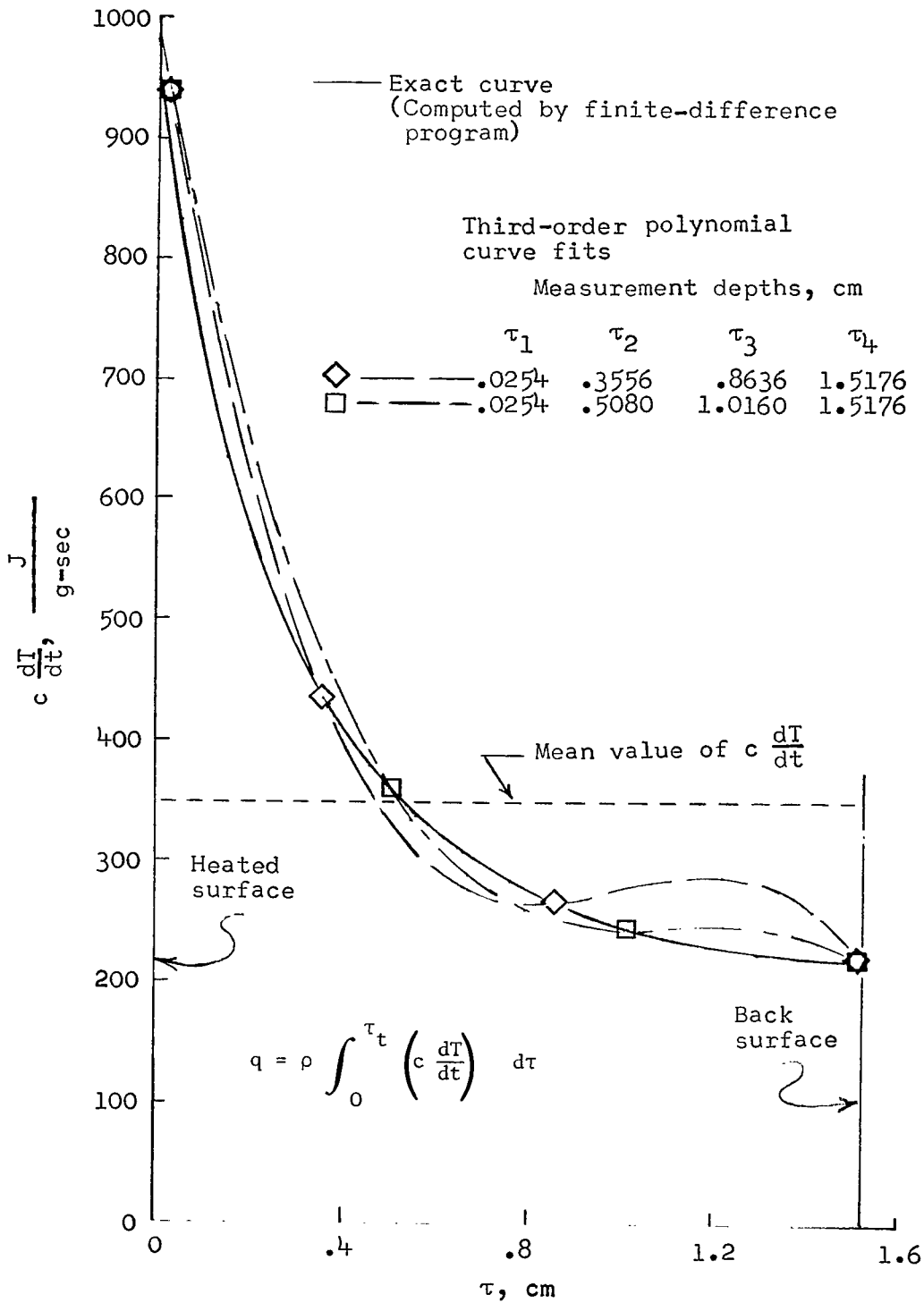


Figure 11.- Comparison of exact variation of $c \frac{dT}{dt}$ through wall with integral-method curve fits at 11 sec for $q = 1022$ watts/cm² and $\tau_t = 1.524$ cm.

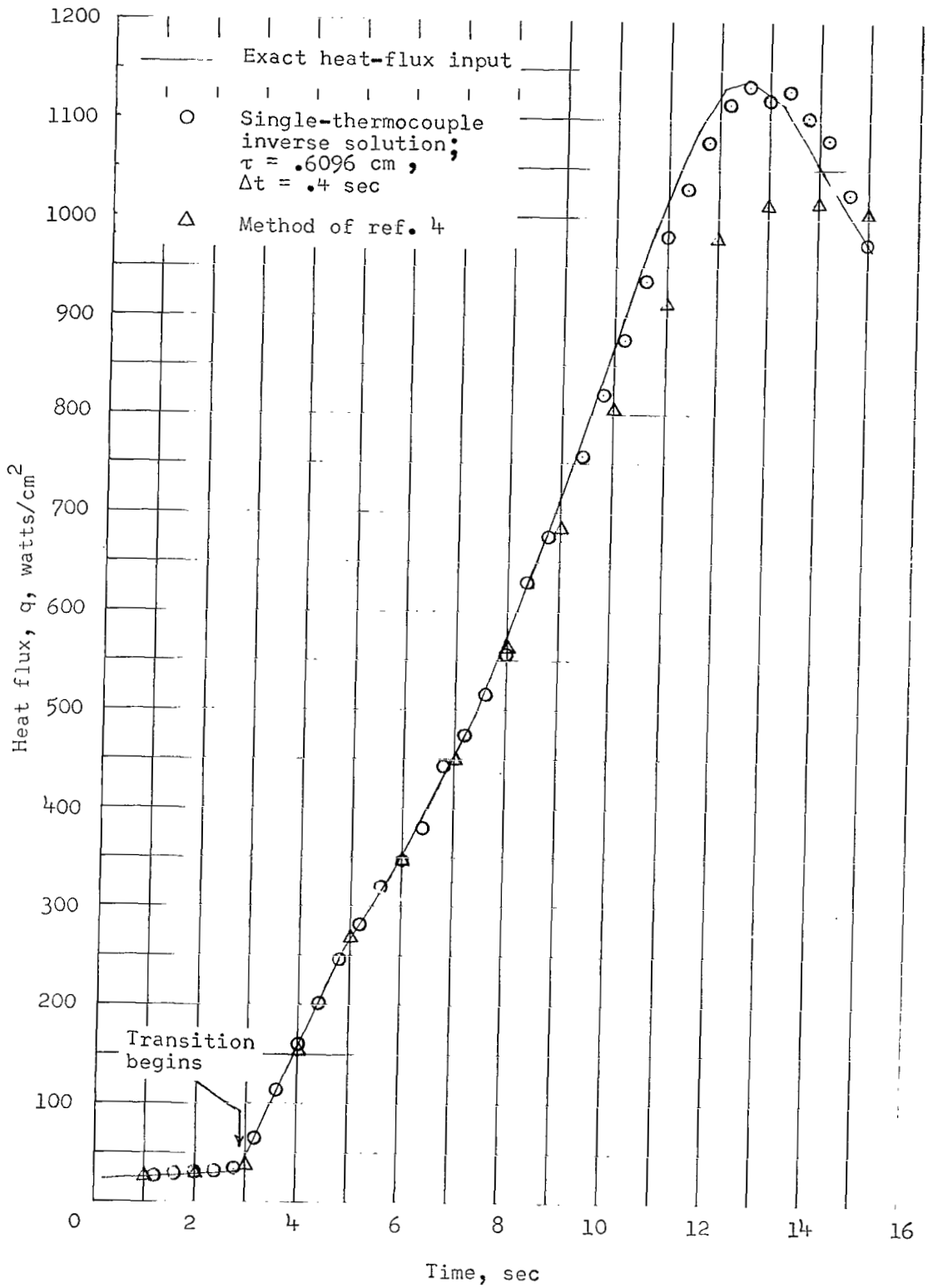


Figure 12.- Solution by method of reference 4 compared with the exact input and with the single-thermocouple inverse solution.
 $\tau = 0.6096$ cm; $\tau_t = 1.524$ cm.

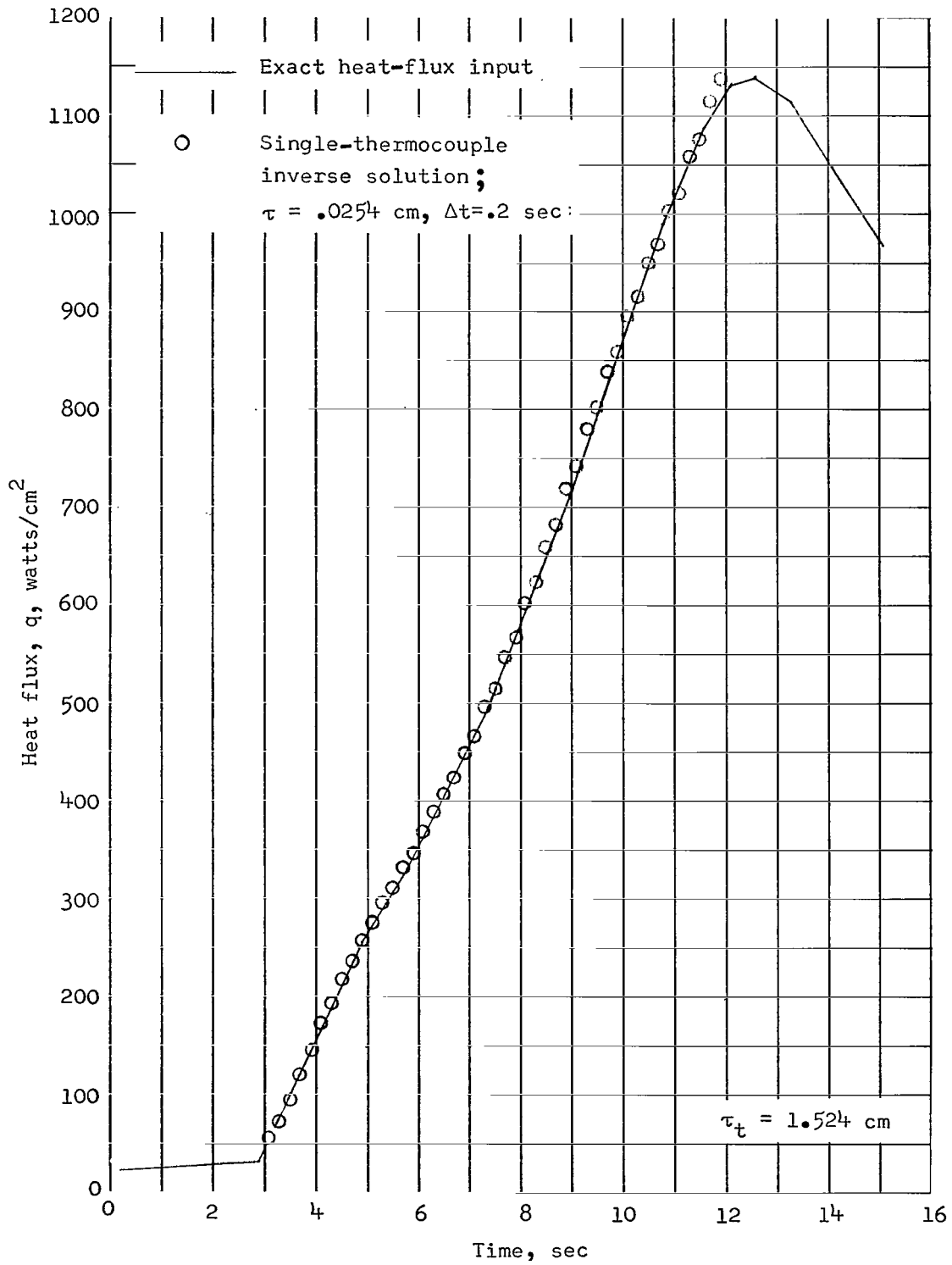


Figure 13.- Single-thermocouple inverse solution obtained by fitting a sixth-order polynomial to scattered temperature data (3σ of 25° K) compared with exact heat-flux input.

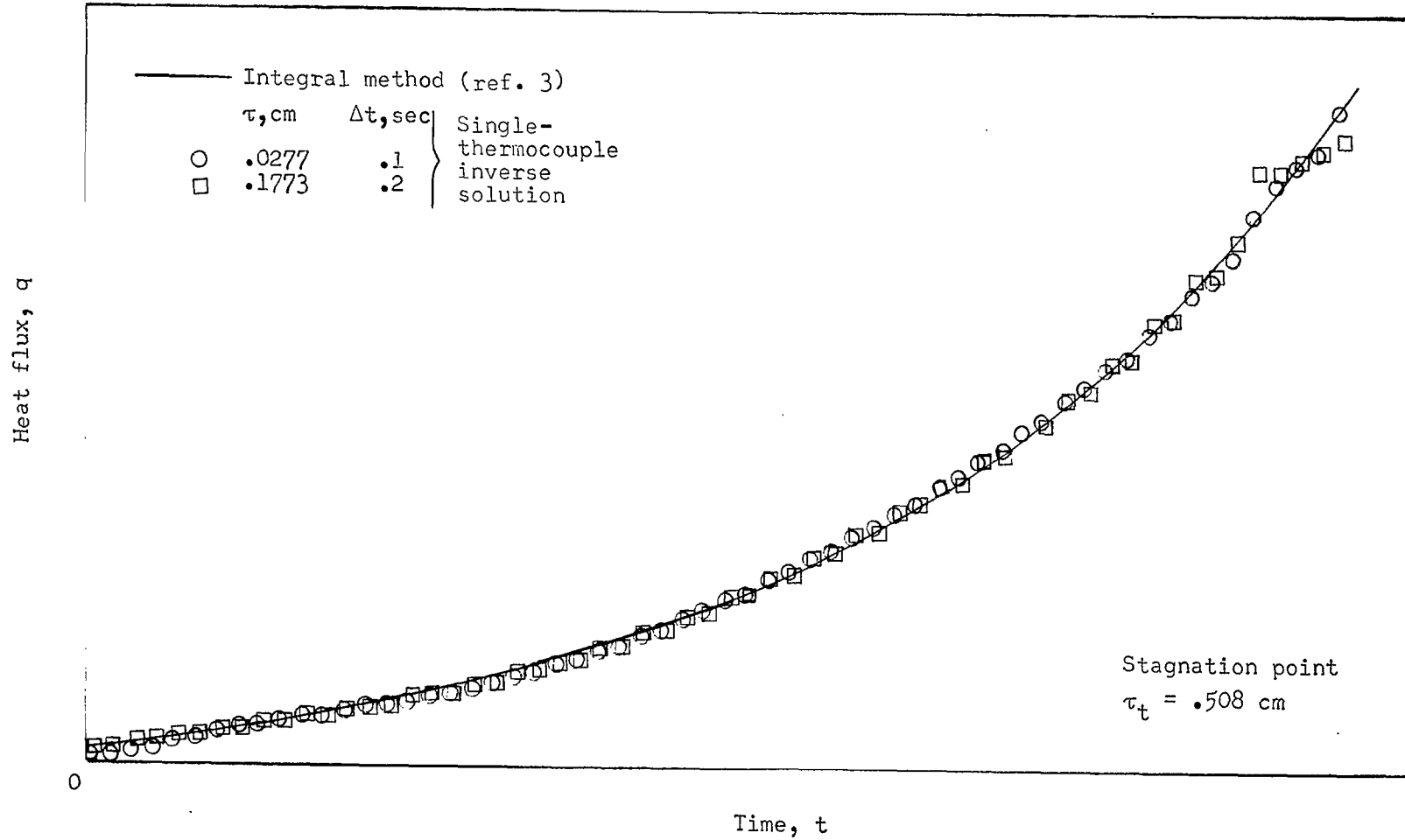


Figure 14.- Comparison of heating rates determined from Fire 11 flight temperature measurements during first data period, as computed by single-thermocouple inverse method and by integral method in reference 3.

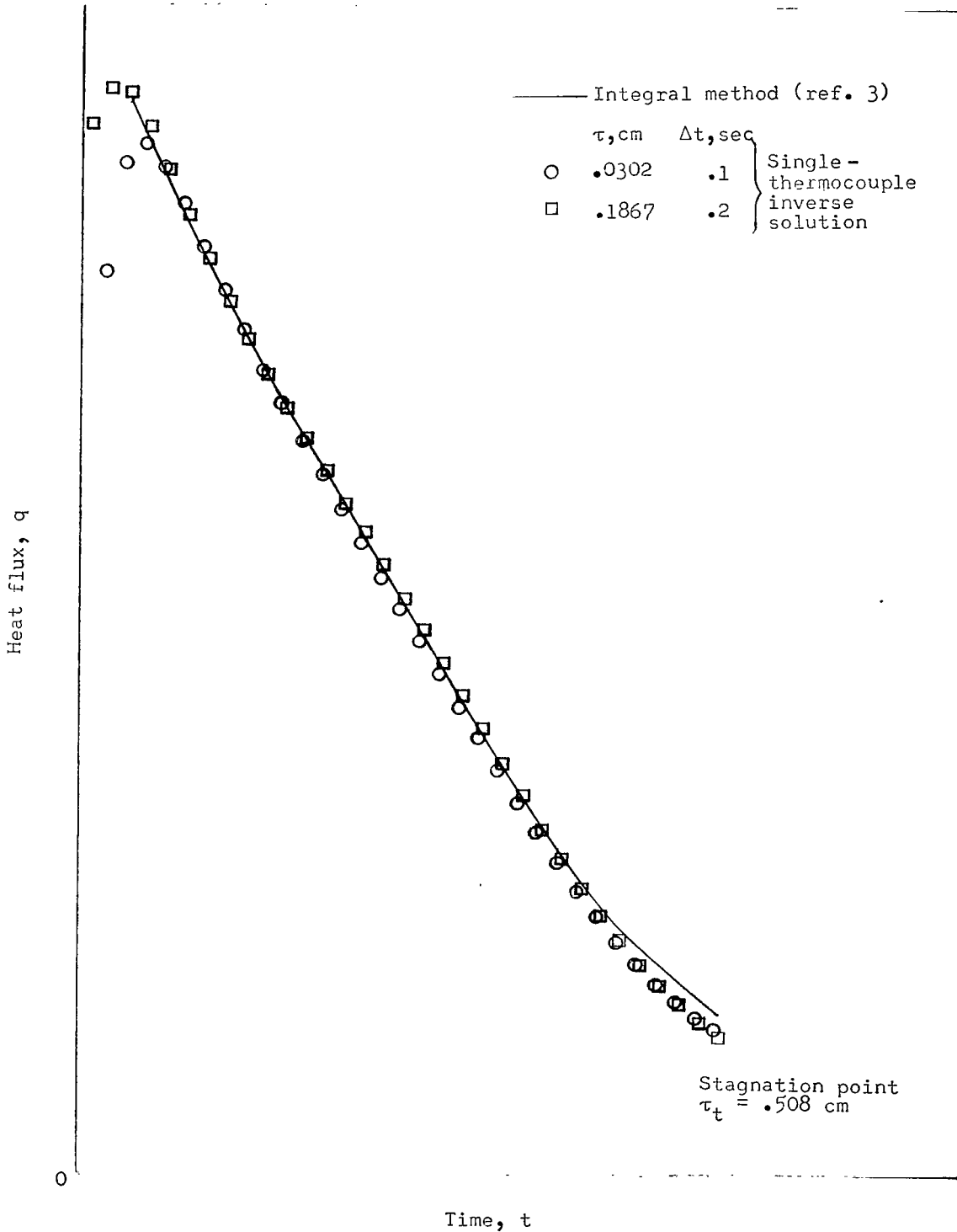
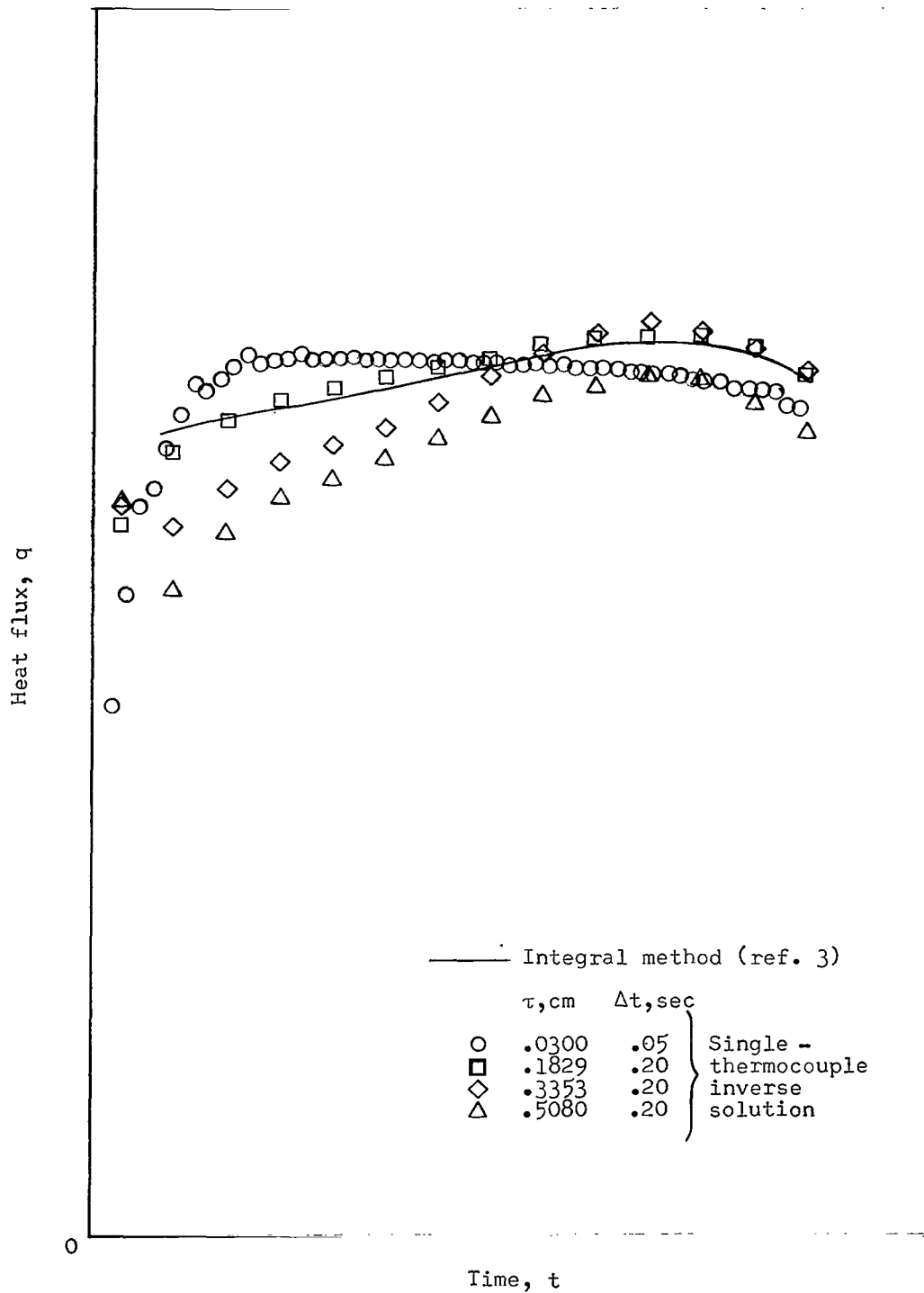
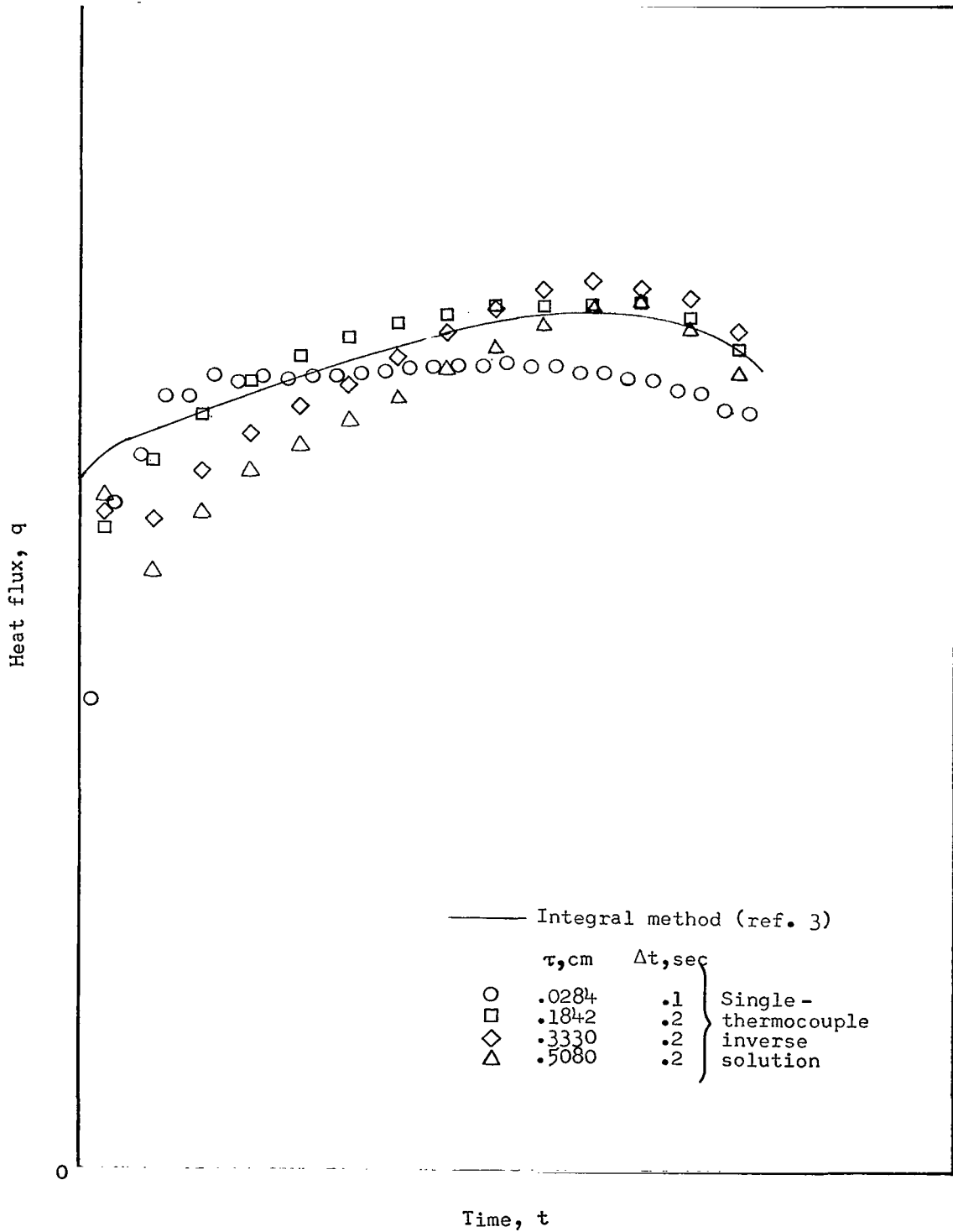


Figure 15.- Comparison of heating rates determined from Fire II flight temperature measurements during third data period, as computed by single-thermocouple inverse method and by integral method in reference 3.



(a) $s/R = 0.54$.

Figure 16.- Comparison of heating rates determined from Fire II flight temperature measurements during second data period, as computed by single-thermocouple inverse method and by integral method in reference 3. $\tau_t = 0.508$ cm.



(b) $s/R = 0.90$.

Figure 16.- Concluded.

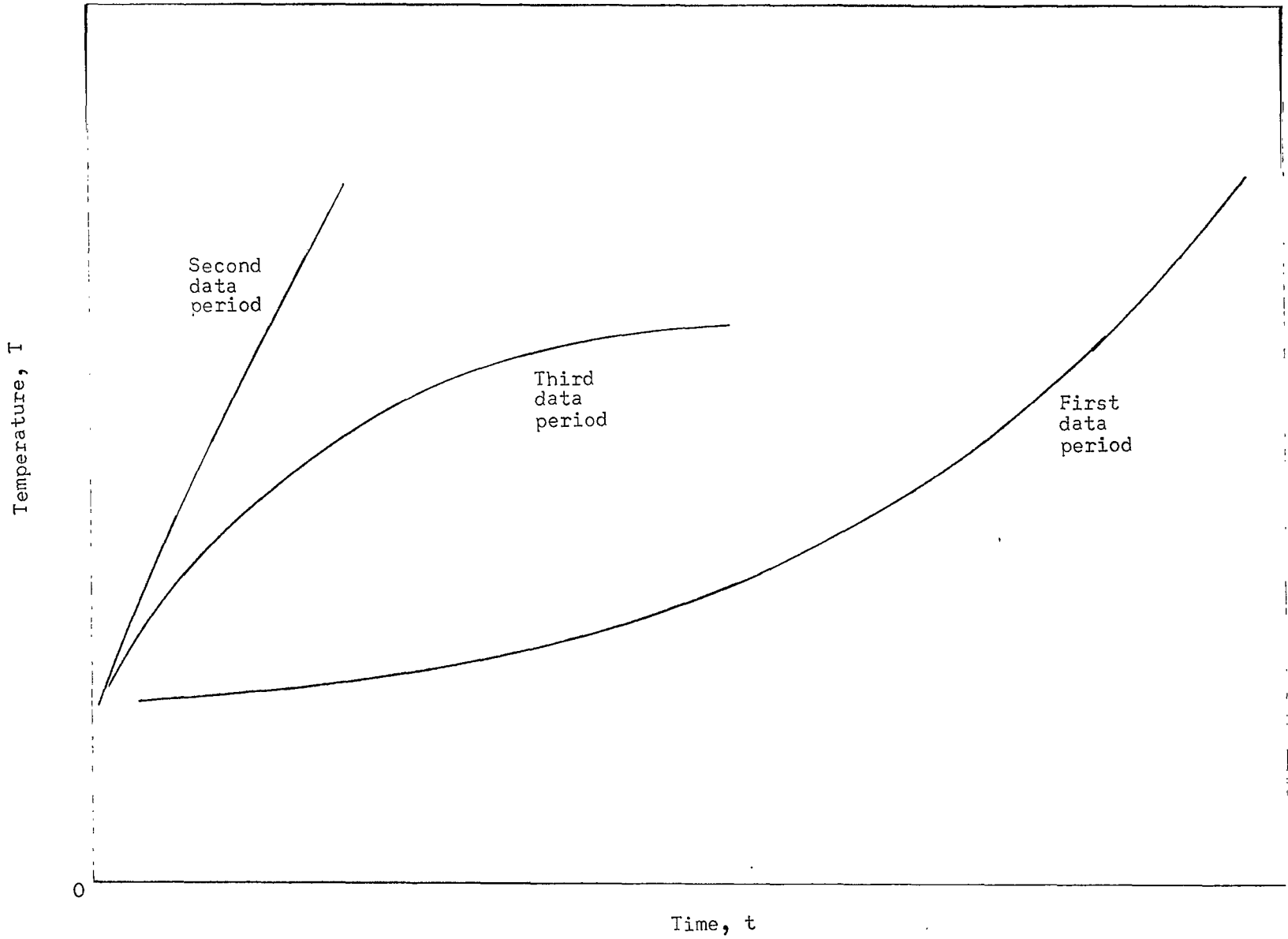


Figure 17.- Comparison of temperature rise for the three data periods of the Fire II spacecraft (ref. 3).

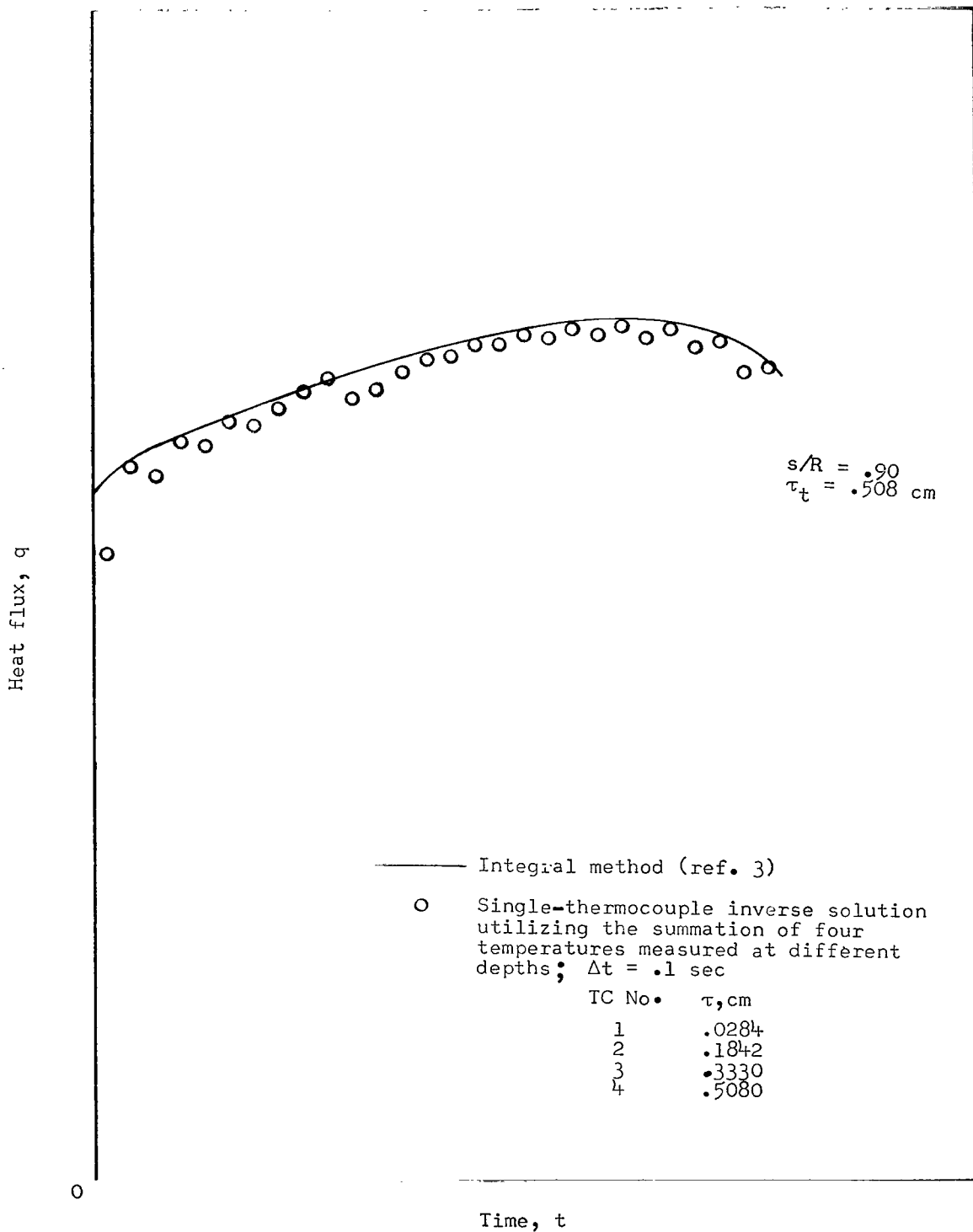


Figure 18.- Comparison of heating rates determined from Fire II flight temperature measurements during second data period, as computed by single-thermocouple inverse method utilizing multiple-thermocouple data and by integral method in reference 3.

FIRST CLASS MAIL

070 001 50 51 305 68226 00903
AIR FORCE WEAPONS LABORATORY/AFWL/
KIRTLAND AIR FORCE BASE, NEW MEXICO 87117

ALL INFORMATION CONTAINED HEREIN IS UNCLASSIFIED

POSTMASTER: If Undeliverable (Section 158
Postal Manual) Do Not Return

"The aeronautical and space activities of the United States shall be conducted so as to contribute . . . to the expansion of human knowledge of phenomena in the atmosphere and space. The Administration shall provide for the widest practicable and appropriate dissemination of information concerning its activities and the results thereof."

— NATIONAL AERONAUTICS AND SPACE ACT OF 1958

NASA SCIENTIFIC AND TECHNICAL PUBLICATIONS

TECHNICAL REPORTS: Scientific and technical information considered important, complete, and a lasting contribution to existing knowledge.

TECHNICAL NOTES: Information less broad in scope but nevertheless of importance as a contribution to existing knowledge.

TECHNICAL MEMORANDUMS: Information receiving limited distribution because of preliminary data, security classification, or other reasons.

CONTRACTOR REPORTS: Scientific and technical information generated under a NASA contract or grant and considered an important contribution to existing knowledge.

TECHNICAL TRANSLATIONS: Information published in a foreign language considered to merit NASA distribution in English.

SPECIAL PUBLICATIONS: Information derived from or of value to NASA activities. Publications include conference proceedings, monographs, data compilations, handbooks, sourcebooks, and special bibliographies.

TECHNOLOGY UTILIZATION PUBLICATIONS: Information on technology used by NASA that may be of particular interest in commercial and other non-aerospace applications. Publications include Tech Briefs, Technology Utilization Reports and Notes, and Technology Surveys.

Details on the availability of these publications may be obtained from:

SCIENTIFIC AND TECHNICAL INFORMATION DIVISION
NATIONAL AERONAUTICS AND SPACE ADMINISTRATION
Washington, D.C. 20546